



Depth must be hidden.
Where?
On the surface.

*Hugo von Hofmannsthal
Austrian poet and essayist*

Avalanche precursors

R. Delannay,

Institut de Physique de Rennes, Université de Rennes 1, CNRS UMR 6251

IPR : S. Kiesgen de Richter, M. Duranteau, N. Brodu, G. Le Caër, P. Richard

LAUM : V. tournat

Russia : V. Zaitsev

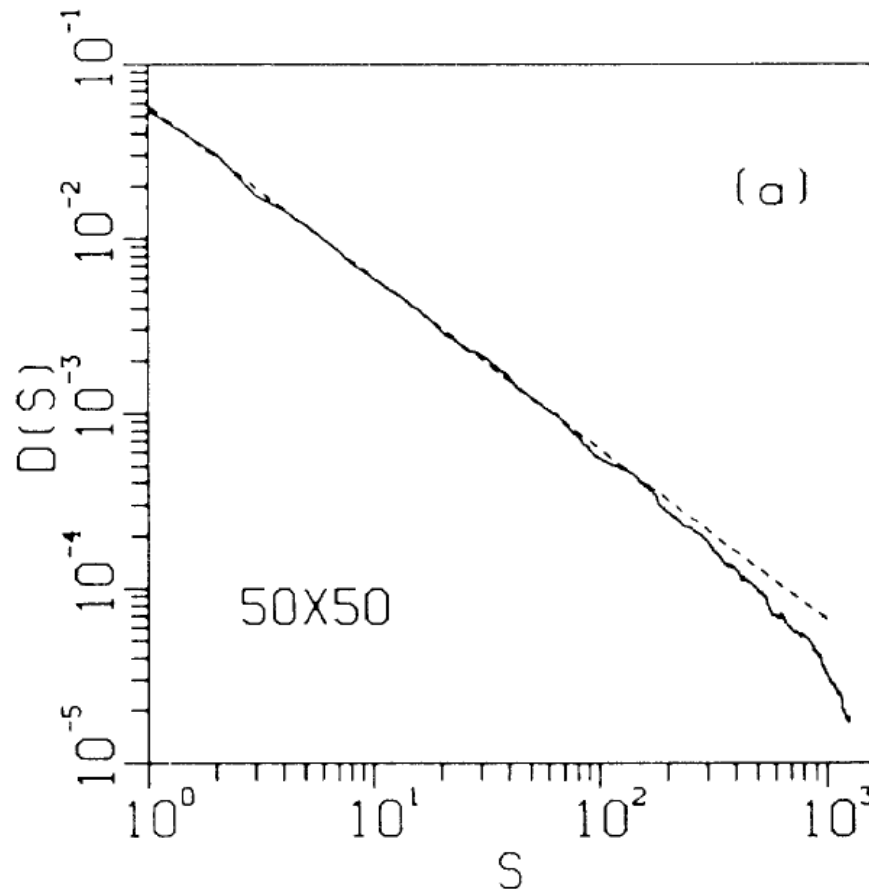
Introduction

- 1987 : P. Bak, C. Tang, K. Wiesenfeld, Phys. Rev. Lett. 59, 381
 - Introduce the concept of self organized criticality
 - Uses sand piles to illustrate this concept : when its slope reaches a critical value where the system is barely stable with respect to small perturbations.
 - Performed numerical simulations with a 2D cellular automaton describing the interaction of an integer variable z (local slope) with its nearest neighbors :

$$\text{Si } z > K \Rightarrow \begin{cases} z(x,y) \rightarrow z(x,y) - 4, \\ z(x \pm 1,y) \rightarrow z(x \pm 1,y) + 1, \\ z(x,y \pm 1) \rightarrow z(x,y \pm 1) + 1, \end{cases}$$

- System is set up with random initial conditions $z \gg K$, then it simply evolves until it stops.
- The dynamics is then probed by measurement of the response to small local random perturbations : the tripping of a site originate a cluster of affected sites through a domino process.

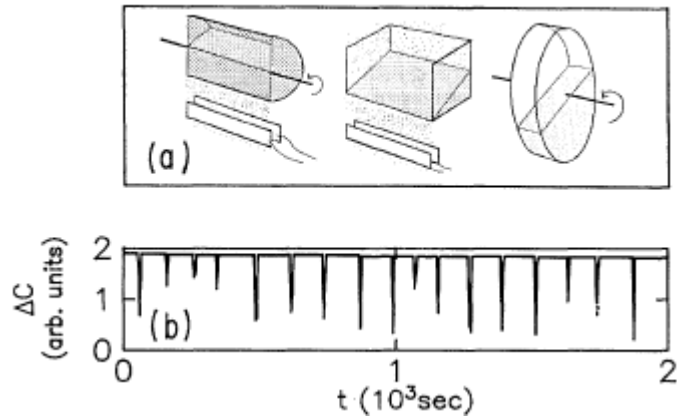
Distribution of cluster sizes



$$D(s) \sim s^{-\tau}, \tau \approx 0.98$$

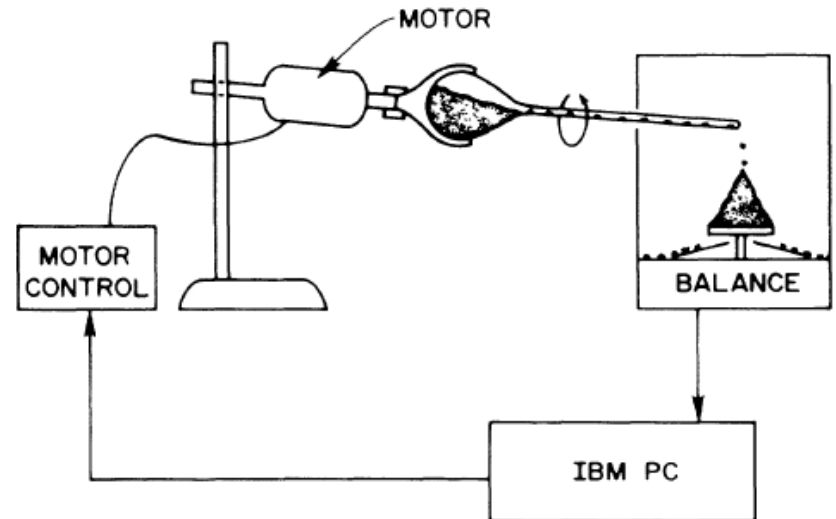
First experiments

- H. M. Jaeger et al. Phys. Rev. Lett. 62, 40 (1989)

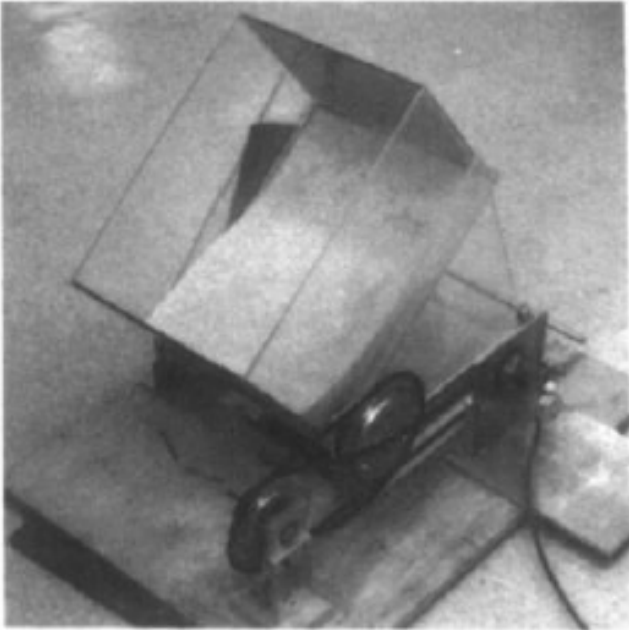


These experiments measured only the events inducing flow past the rim of the sandpile and not those occurring totally within the pile

- G. A. Held et al. Phys. Rev. Lett. 65, 1120 (1990), J. Rosendhal et al. Phys. Rev. Lett. 73, 537 (1994).



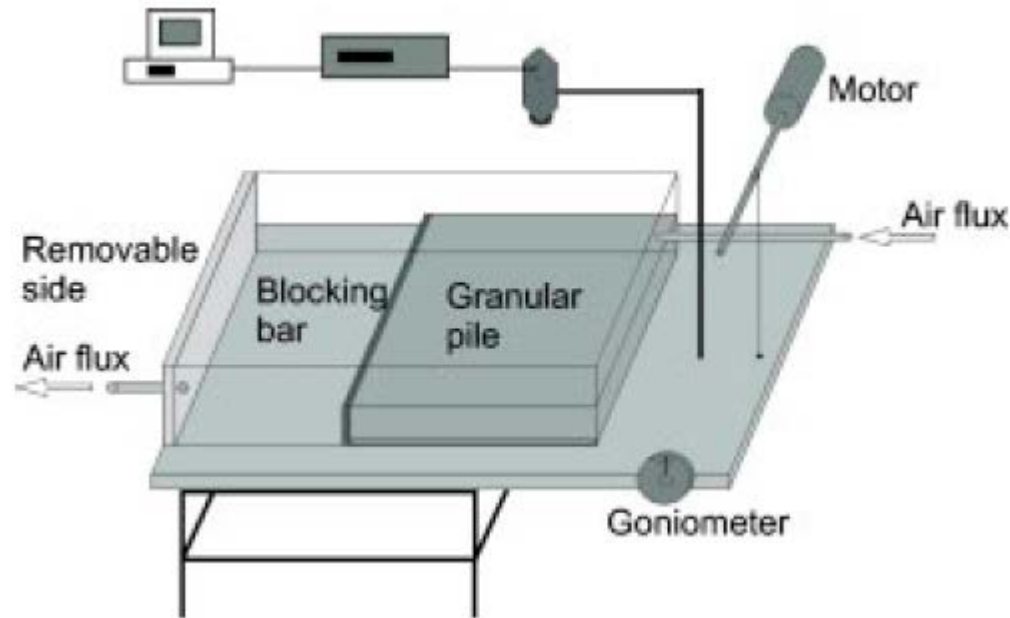
M. Bretz et al. Phys. Rev. Lett. 69, 2431 (1992)



2mm diameter beads

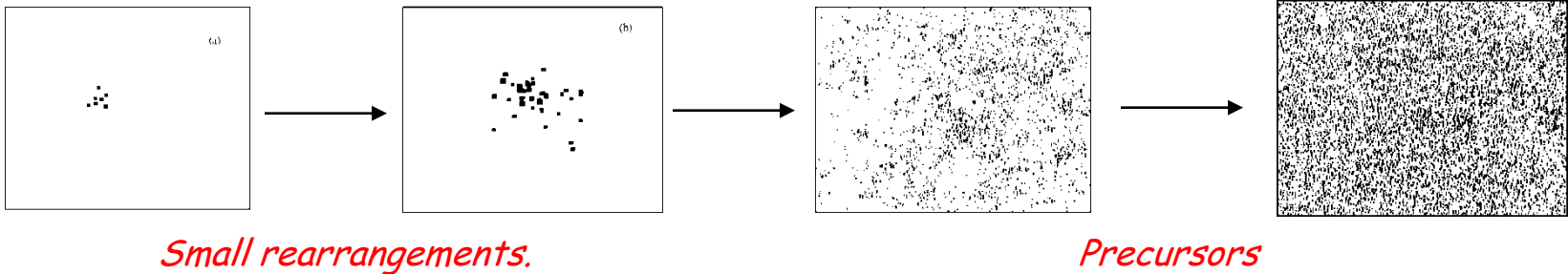
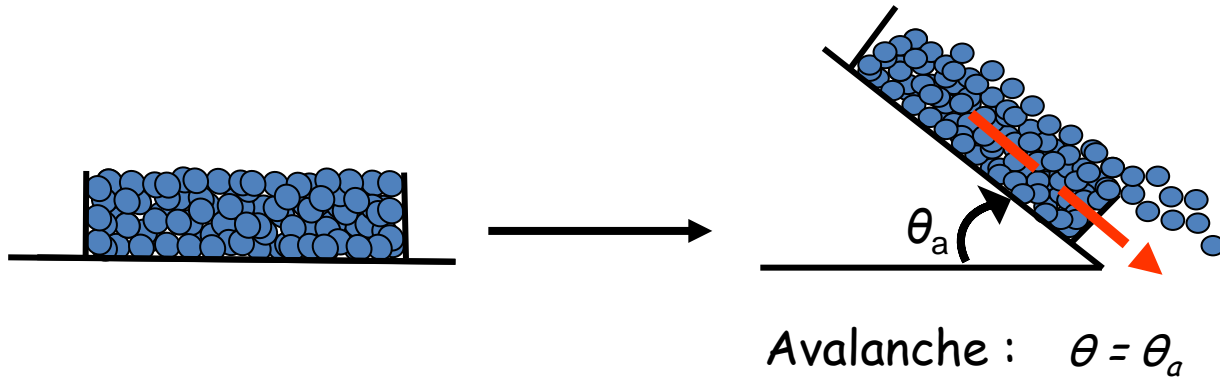
- Initial state prepared by rotating the box until the rough substrate (glued beads) begin to appear at the top of the tray after some avalanches.
- 4 or 5 large avalanches then observed during the slow inclination of the box : rotation rate of 0.22deg/min
- These large slides are separated by a sequence of small “avalanches” which are recorded by a camera.

N. Nérone et al. Physica A 283 (2000) et Phys. Rev. E 67 (2003)



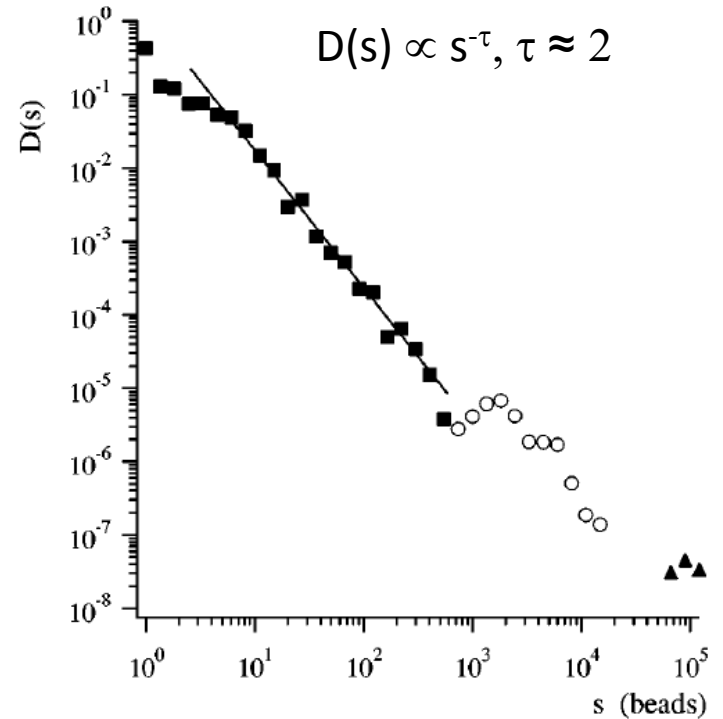
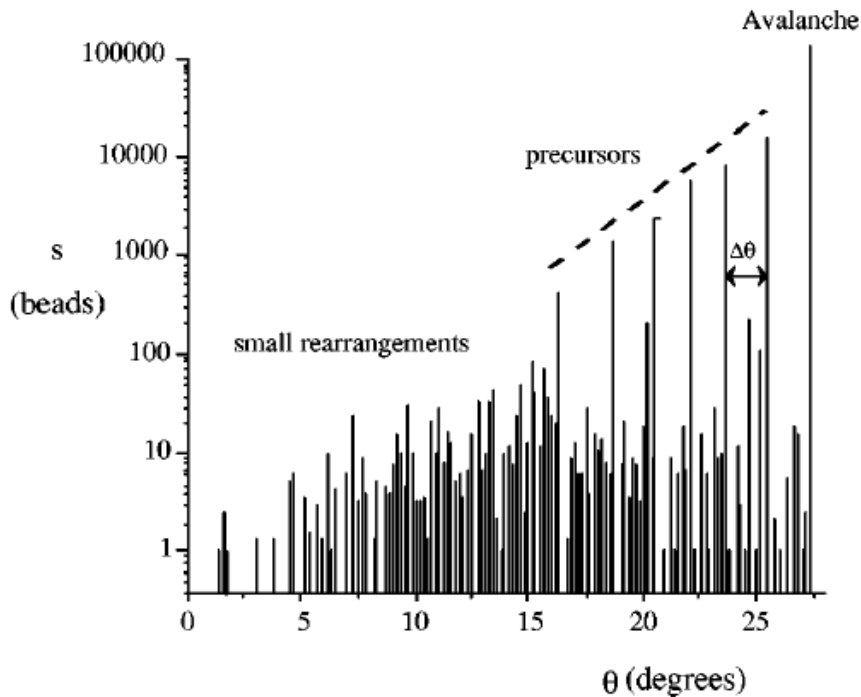
- ~2.2 mm diameter glass beads, box size : 320 mm * 260 mm
- After the box is filled, it is slowly inclined up to the avalanche.
- Measurement of surface rearrangements (image processing)

First observations

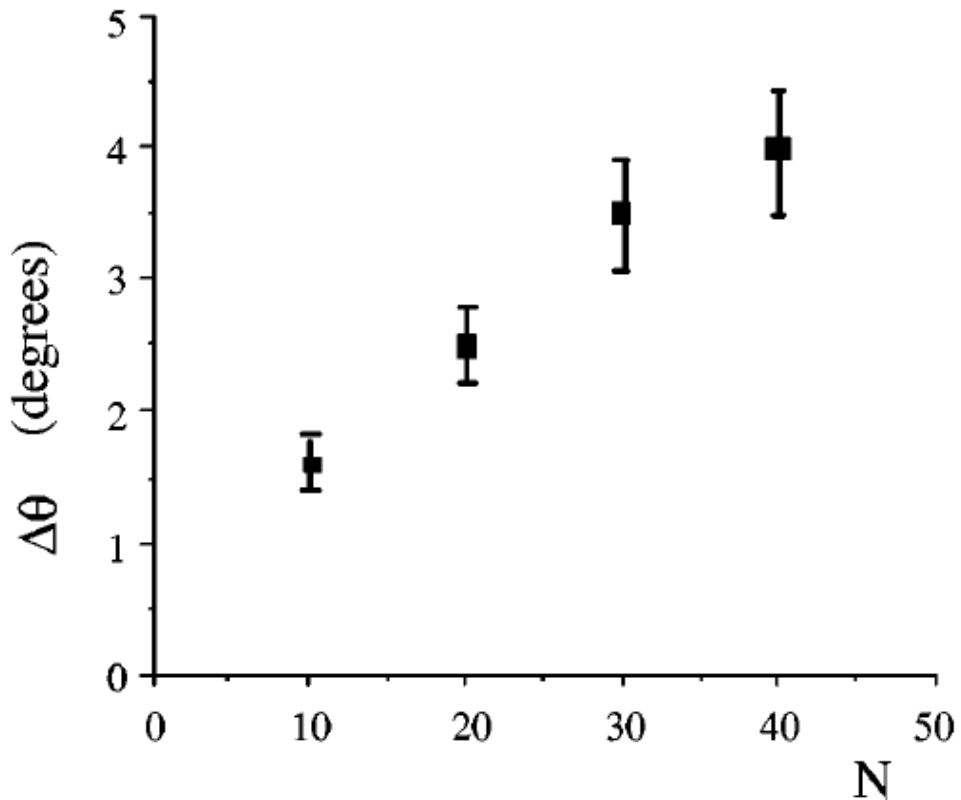


- ❑ Fast and small displacements of surface beads during the whole inclination
- ❑ About 10° before the avalanche, large events occur at approximately regular angular intervals $\Delta\theta$.
- ❑ The beads involved in these so called precursors are uniformly distributed on the free surface.
- ❑ The slope doesn't change before the avalanche.

Rearrangement size distribution function

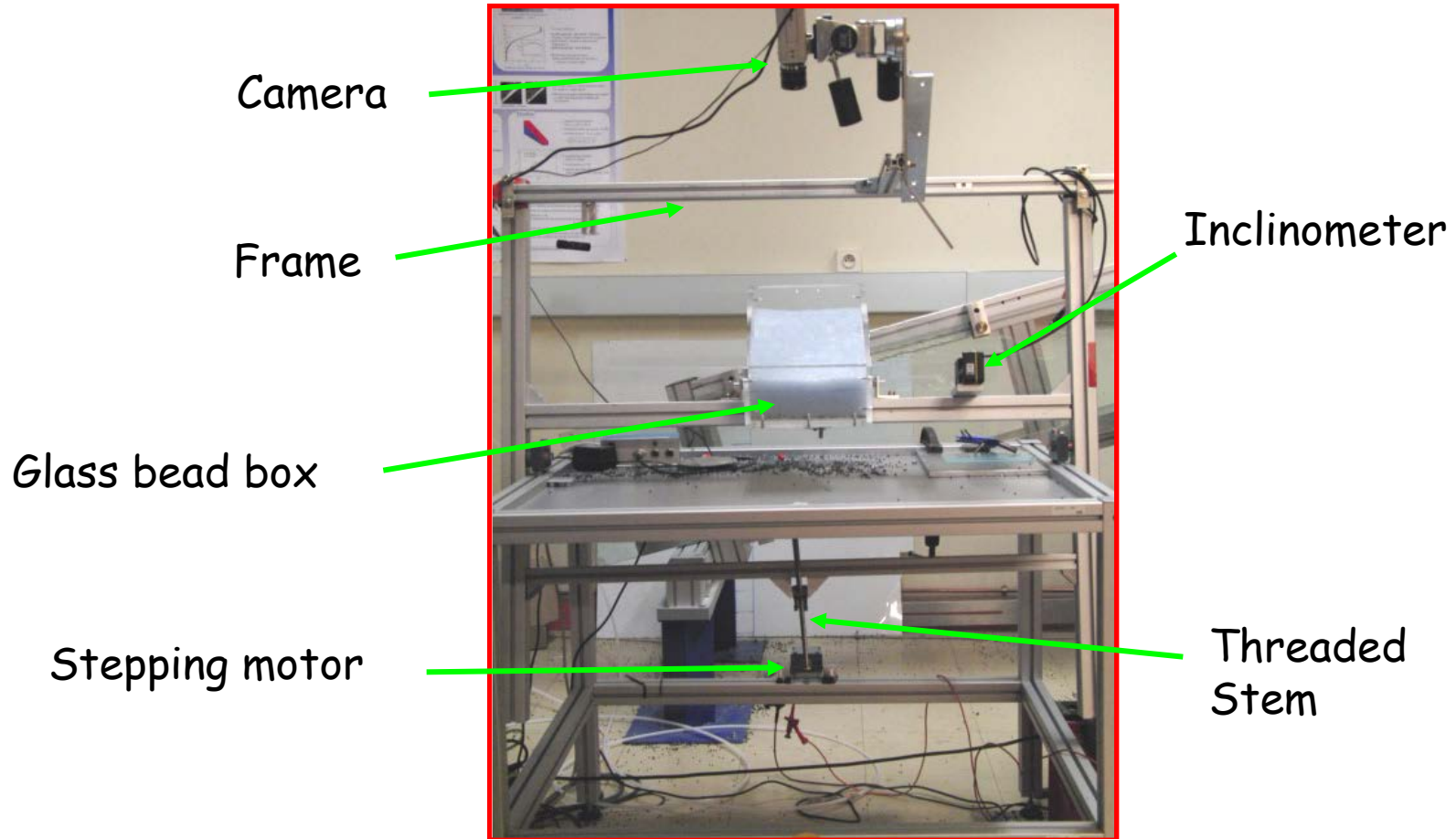


- Size of the events as a function of the inclination angle θ .
- Precursors are triggered at constant intervals $\Delta\theta = 1.8^\circ \pm 0.4^\circ$
- Size distribution function (5 experiments).
- Precursors deviate from the power law : larger probability.



- Variation of the angular interval between successive precursors as a function of the height of the pile (N : number of layers).
- Strong influence of the height : precursors are not superficial events. Collective effects which involve all the bulk.

Experimental set up.



Experimental set up.



Camera

Frame

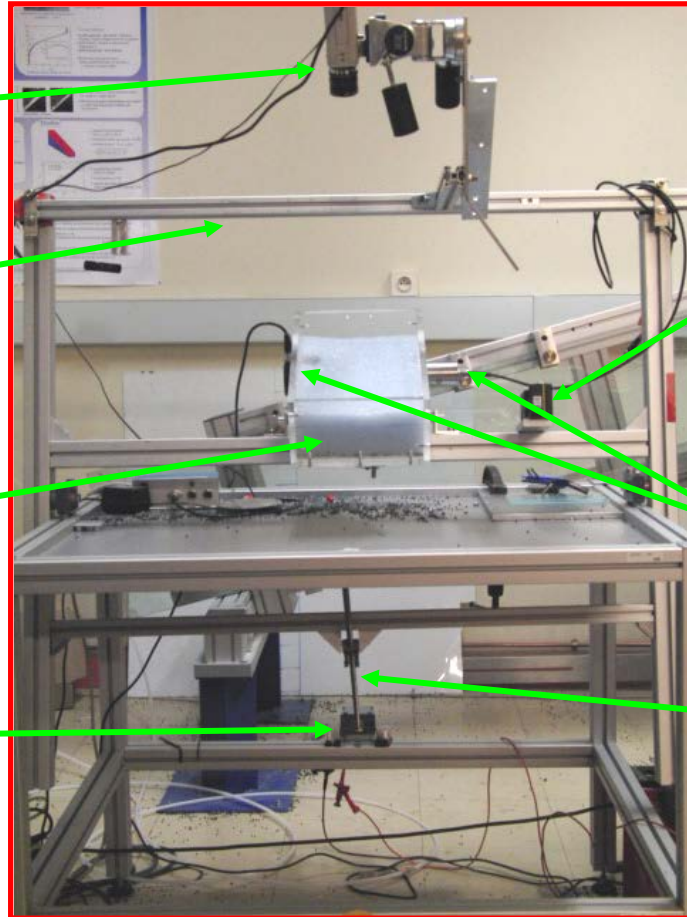
Glass bead box

Stepping motor

Inclinometer

Piezo transducers

Threaded Stem



Some examples of glass beads used



D= 6mm
Transparent beads
Pb : light reflexion



D = 3mm
Black beads
Surface tinted



D = 3mm
Black beads
Volume tinted

Preparation procedure.

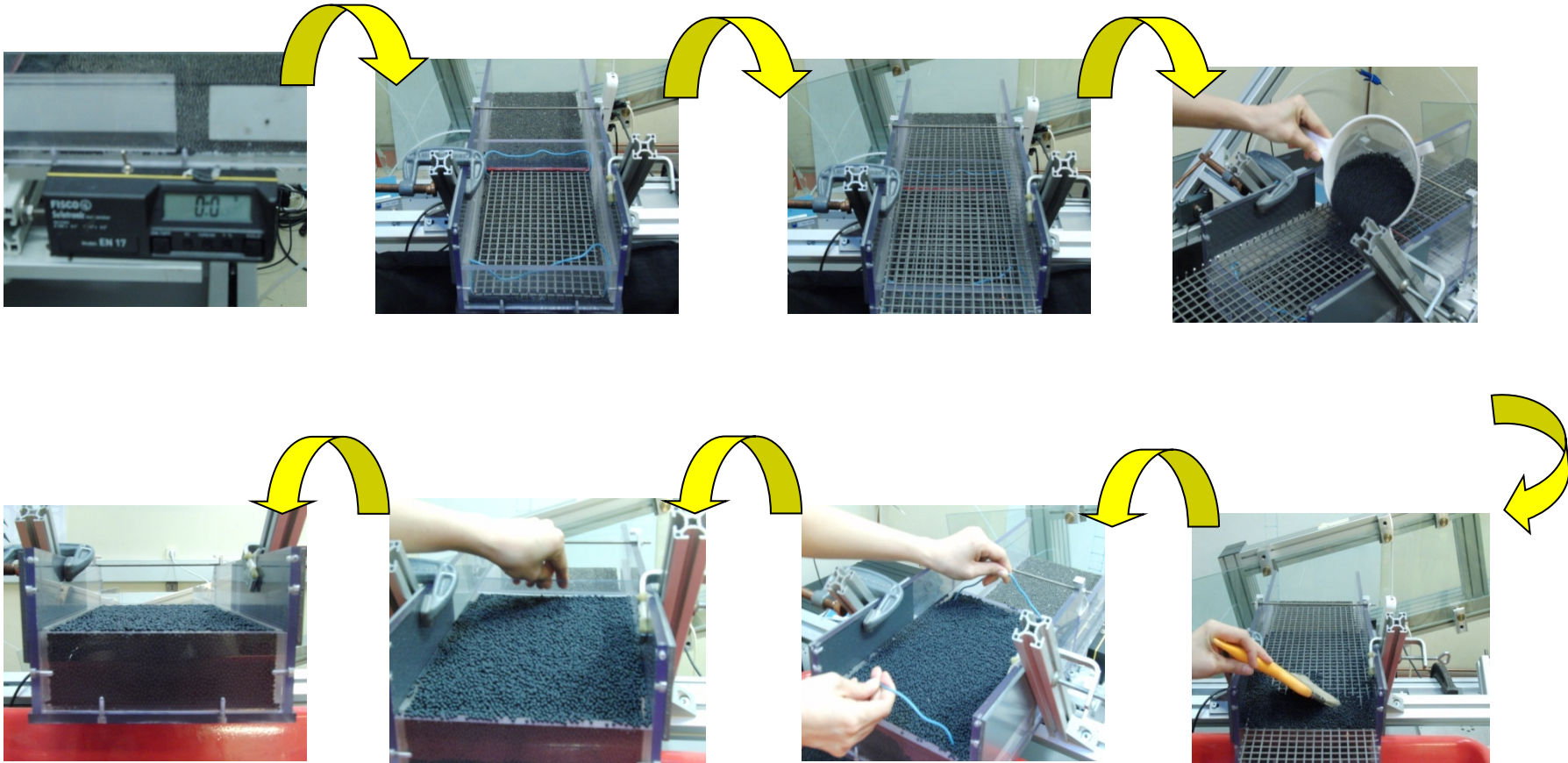
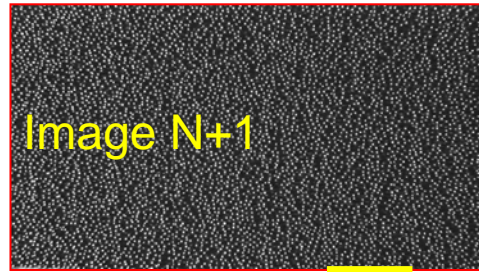
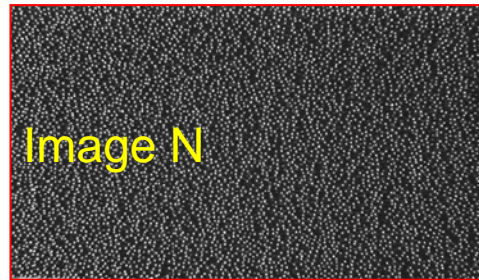
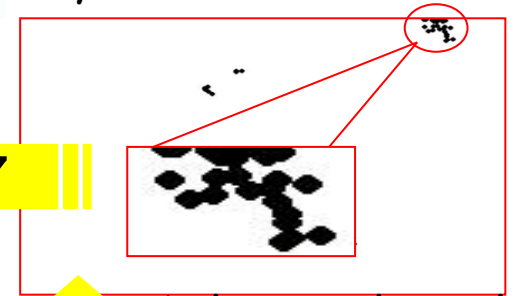
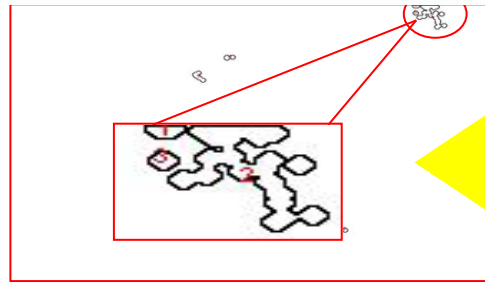


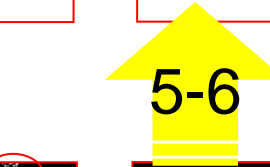
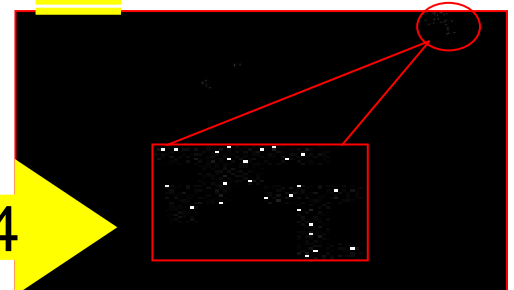
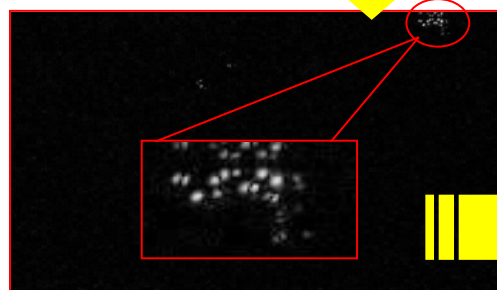
Image processing



Particle analyzer



Substraction of successive images

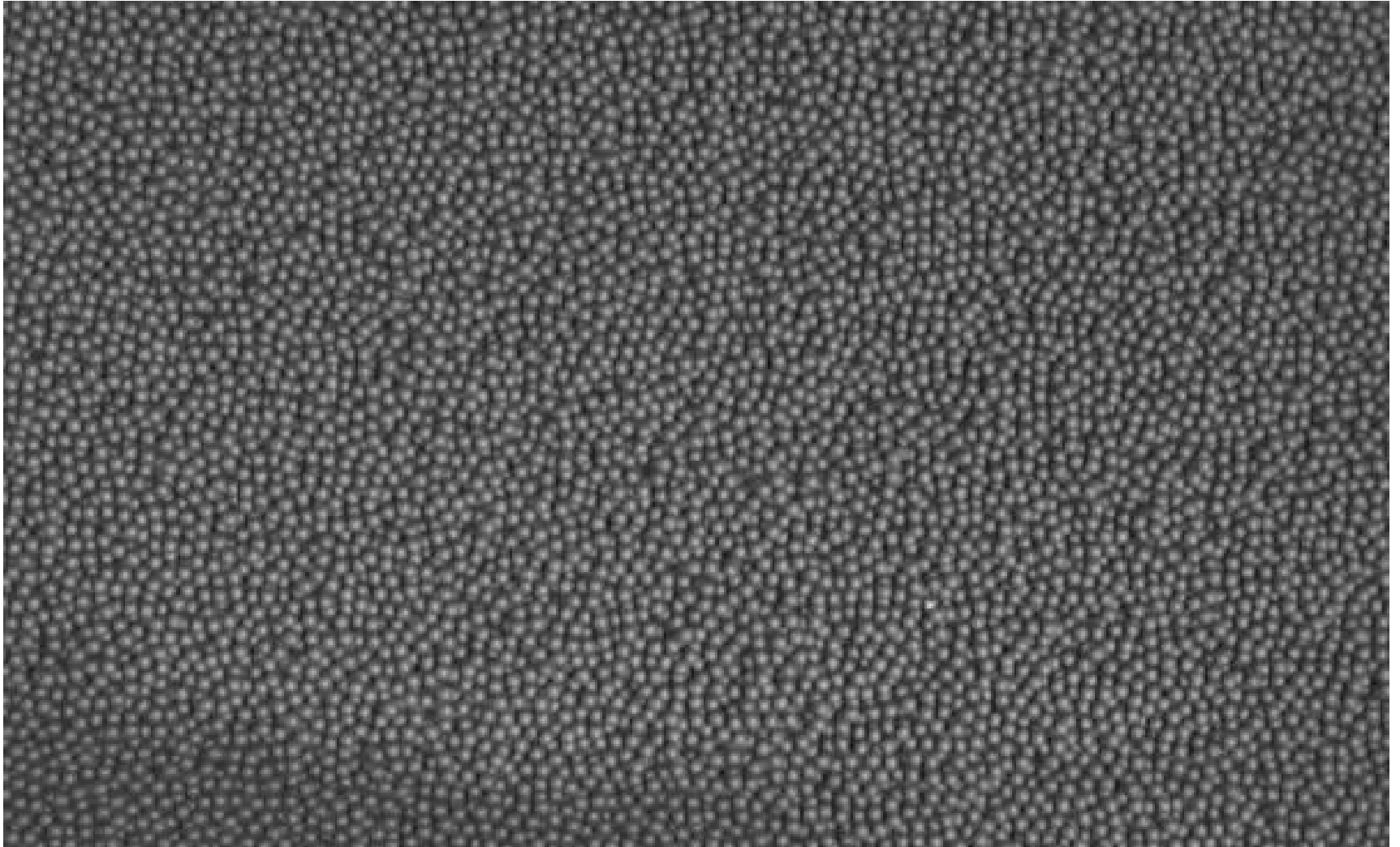


Grey level threshold, binarisation

Extremum (centers)

Dilation algorithm hole-filling

Surface activity



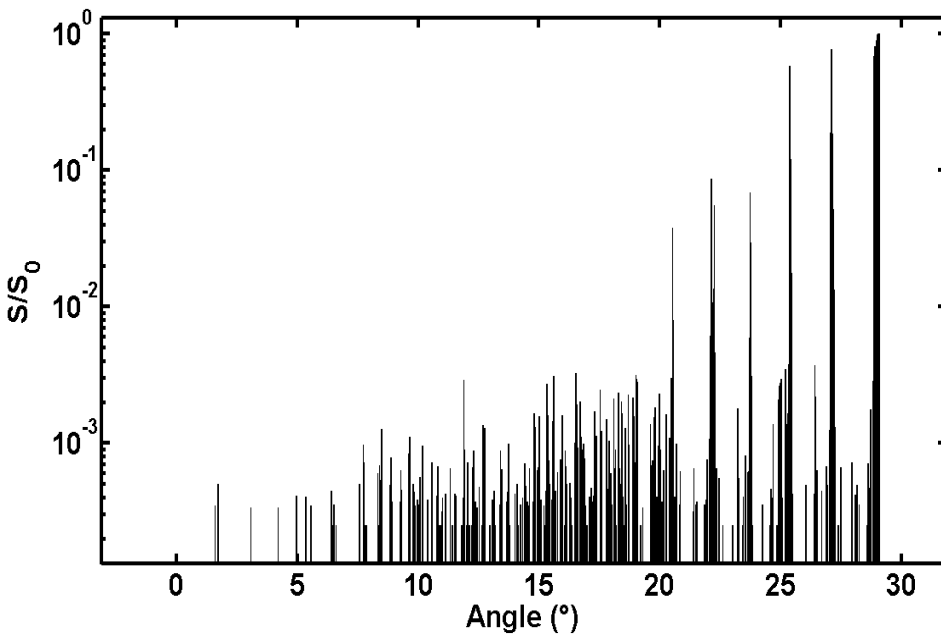
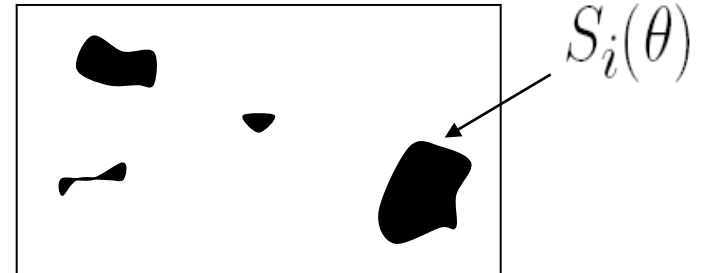
Fraction of rearranged surface

Area of the surface rearranged
between $\theta-d\theta$ and θ

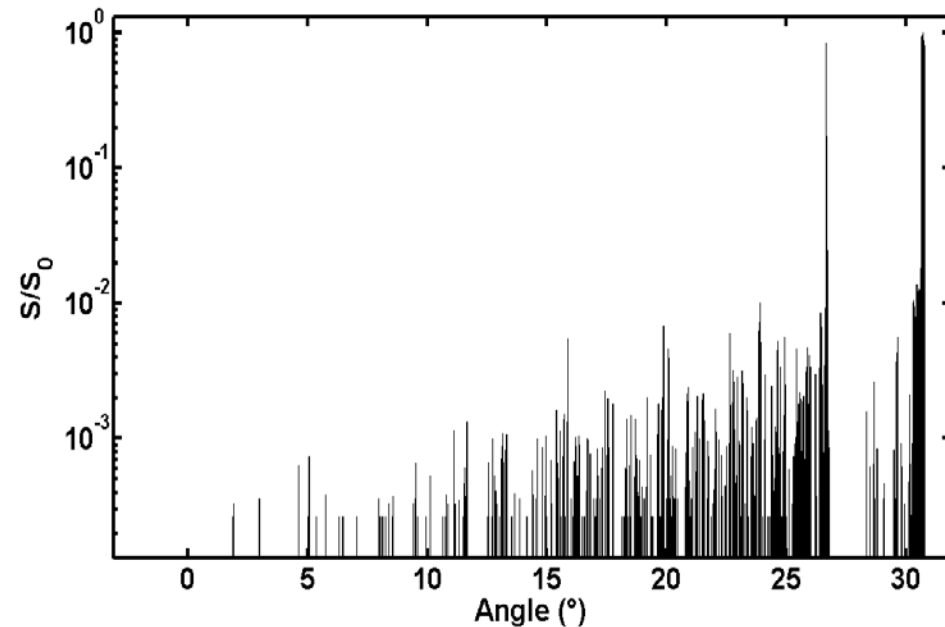
Packing surface
area

$$\frac{S(\theta)}{S_0} = \sum_i \frac{S_i(\theta)}{S_0}$$

Event taking place at surface
between $\theta-d\theta$ and θ



Volume tinted beads



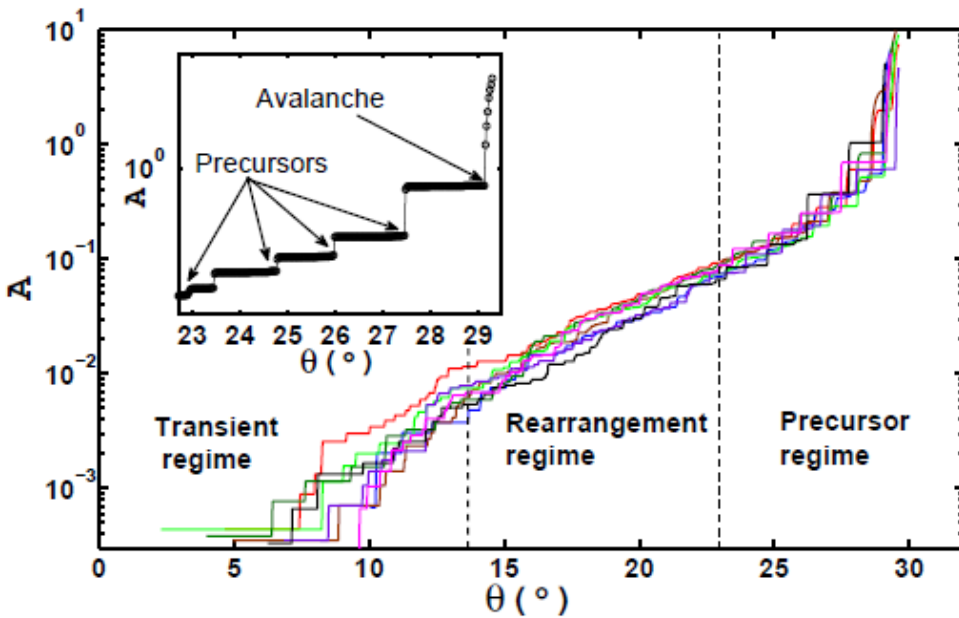
Surface tinted beads

Precursors depend strongly on microscopic details of interactions at grain scale.

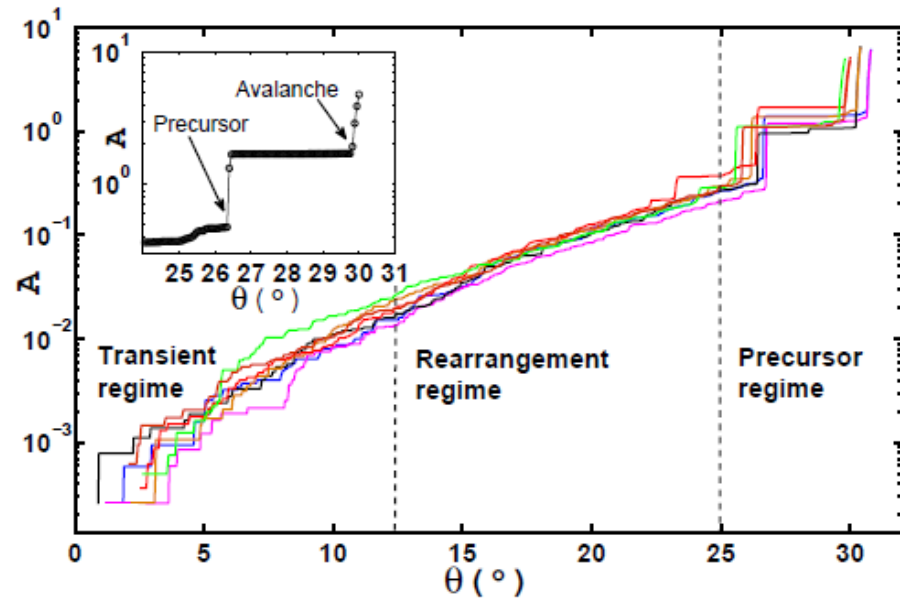
Activity at the surface of the packing.

Surface activity :

$$A(\theta) = \sum_{j=0}^{\left\lfloor \frac{\theta}{d\theta} \right\rfloor} \frac{S(j \cdot d\theta)}{S_0}$$



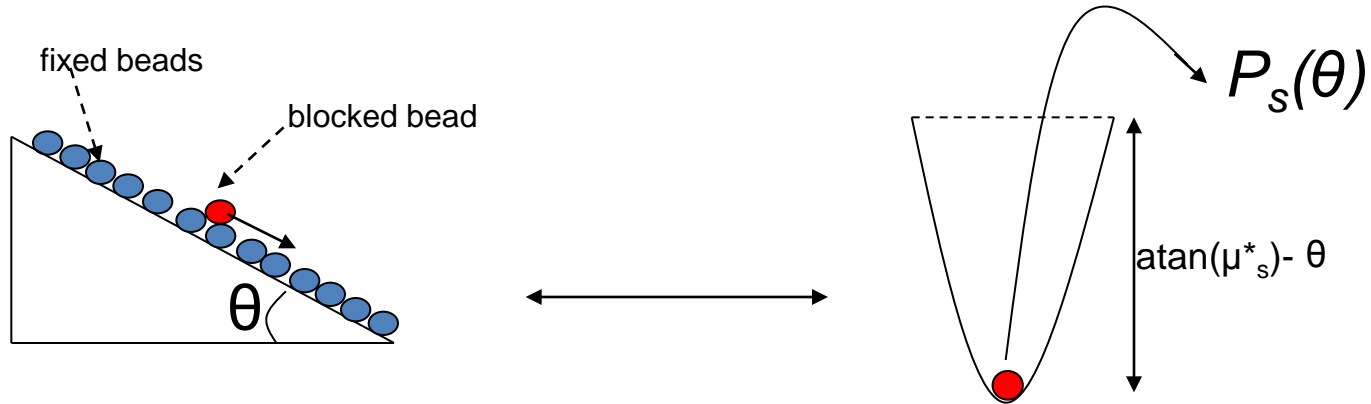
Volume tinted beads



Surface tinted beads

small rearrangement regime

Activation process



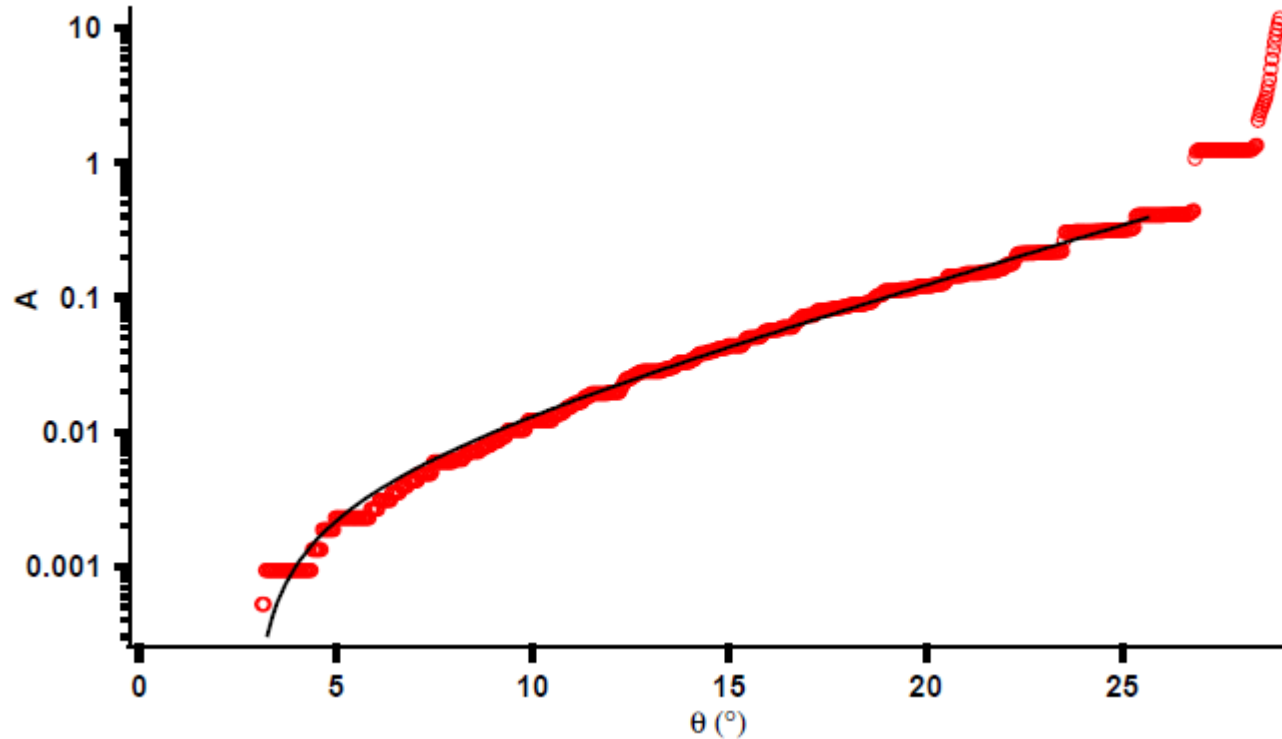
$\vartheta < \text{atan}(\mu_s^*) \longrightarrow$ Blocked

$\vartheta = \text{atan}(\mu_s^*) \longrightarrow$ escape

$$P_s(\theta) = C.e^{-\beta.(\text{atan}(\mu_s^*)-\theta)}$$

$$\left. \begin{aligned} \frac{S(\theta)}{S_0} &= C.e^{(-\beta(\text{atan}(\mu_s^*)-\theta))} \\ A(\theta) &= \int_{\theta_0}^{\theta} \frac{S(u)}{S_0} du \end{aligned} \right\} \boxed{A(\theta) = \frac{K e^{\beta \cdot \theta_0}}{\beta} (e^{\beta(\theta - \theta_0)} - 1)}$$

Small rearrangements régime

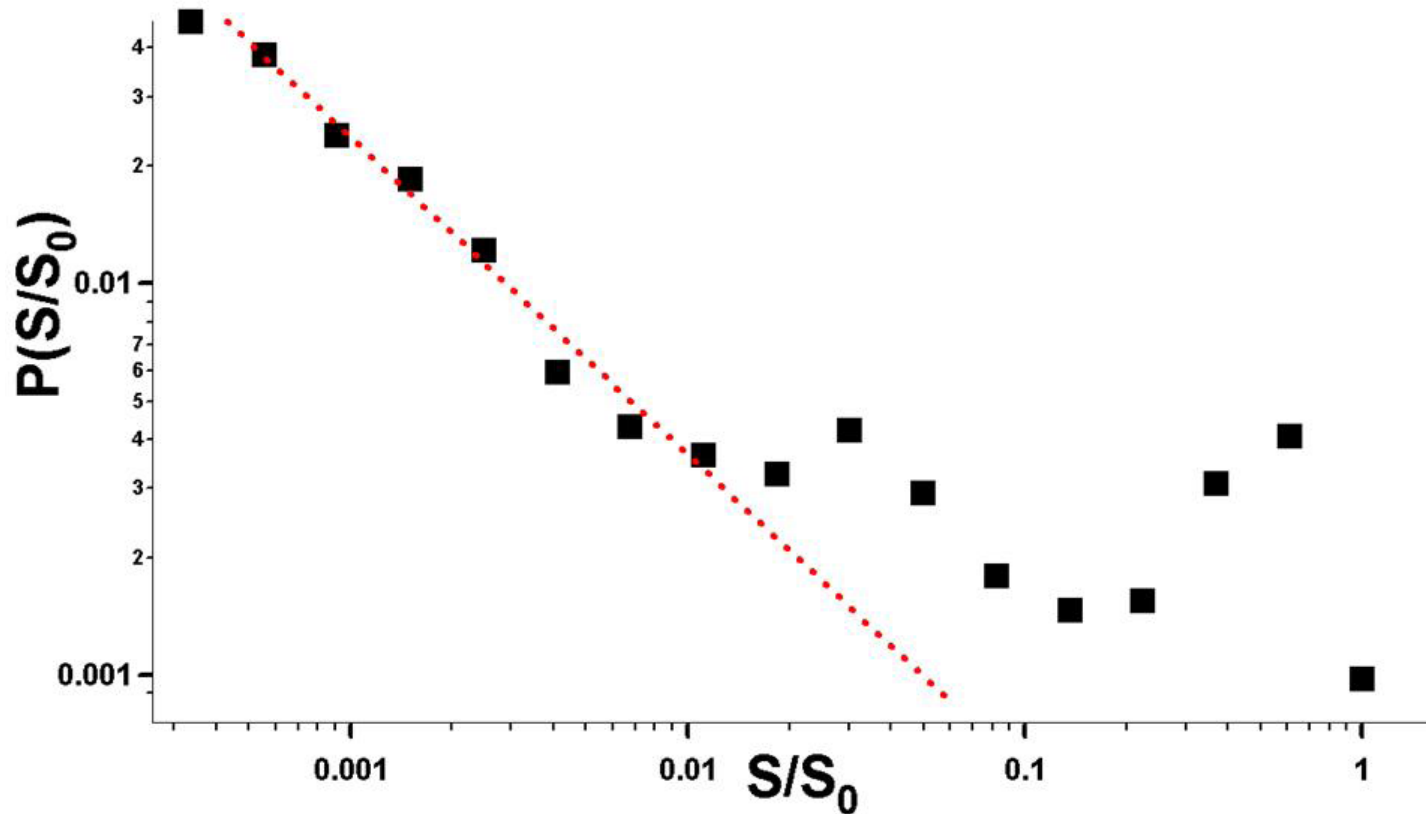


Fit of experimental activity to equation :

$$A(\theta) = \frac{K e^{\beta \cdot \theta_0}}{\beta} (e^{\beta(\theta - \theta_0)} - 1)$$

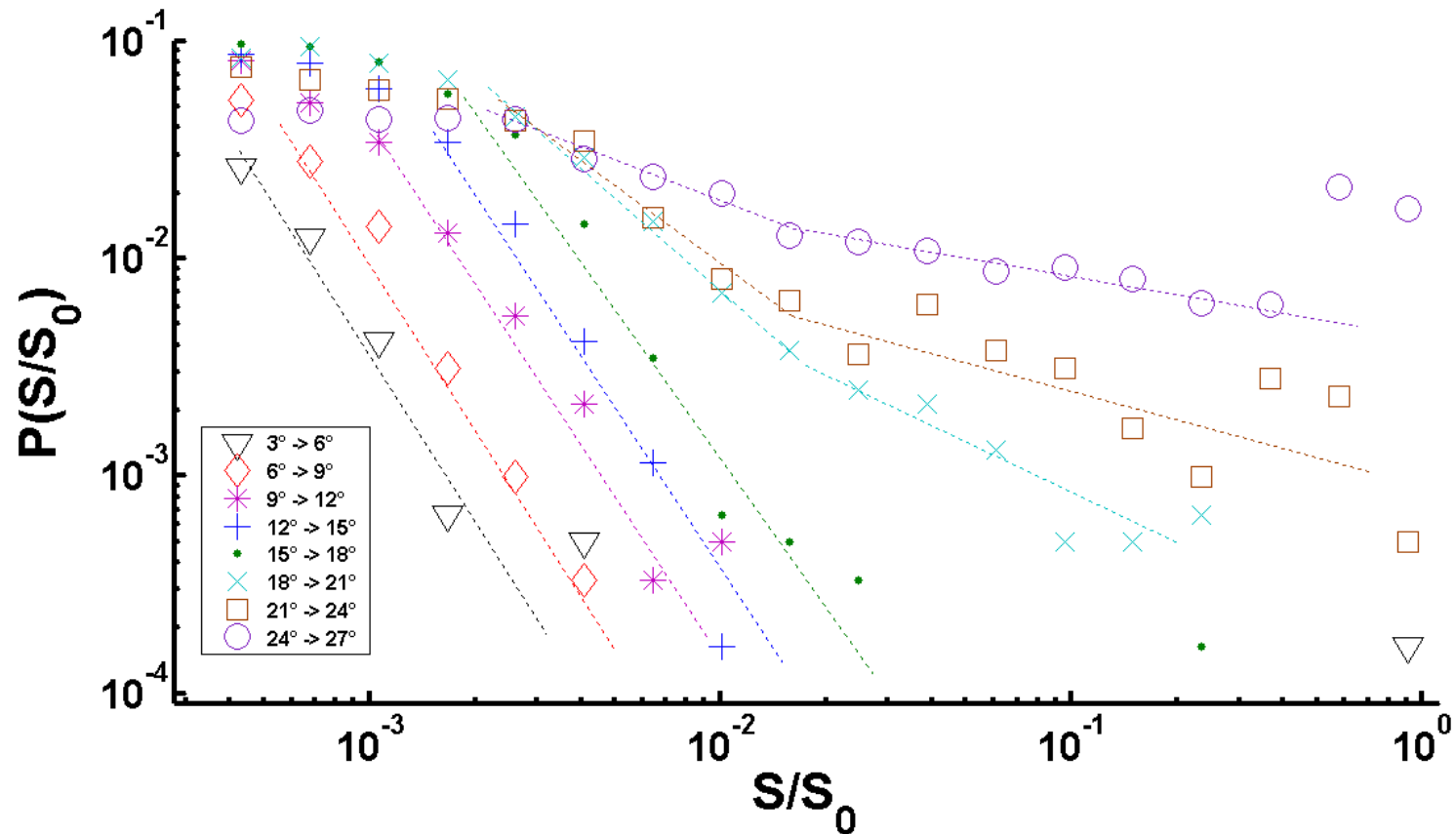
$$\beta = 0.20 \text{ and } \theta_0 = 2.89$$

Distribution of event sizes



Distribution departs from a power law behavior when the precursor regime is reached (excess of large events).

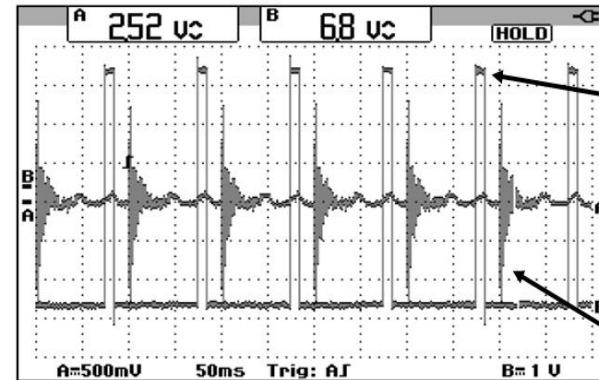
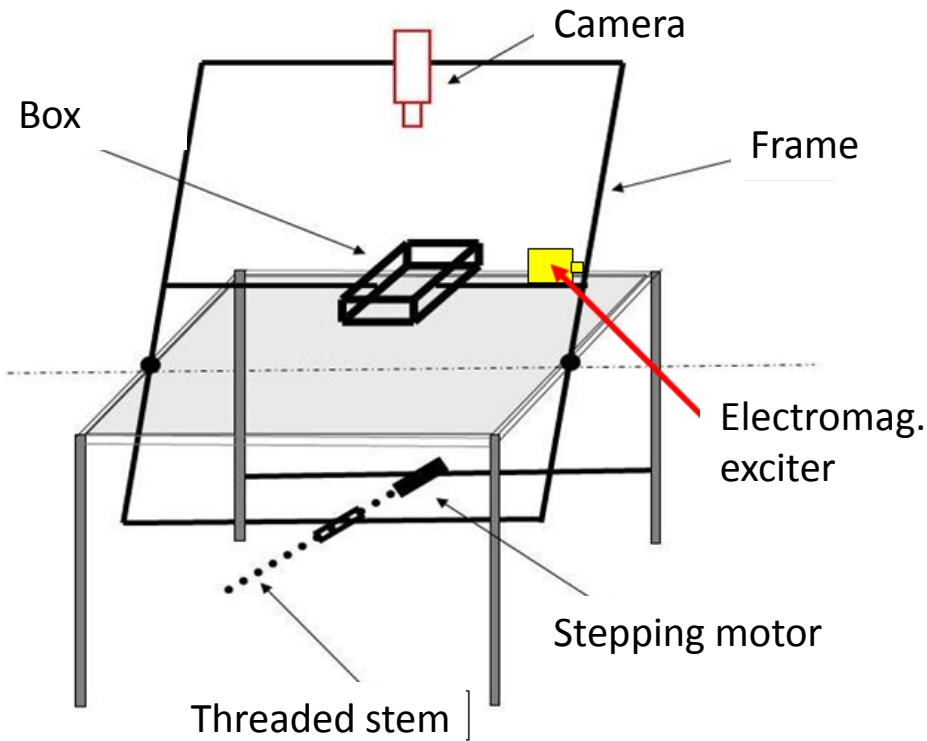
Transition point.



Evolution of the size distribution of events occurring in a window of constant width (3°) with the inclination angle.

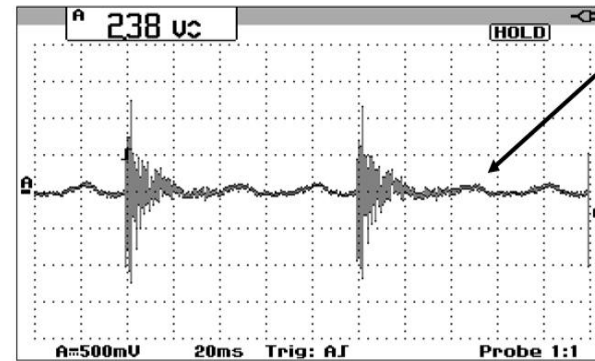
Distributions follow the same power law for $\theta < 18^\circ$. Transition point located near 18° .

Precursor regime : influence of external noise.

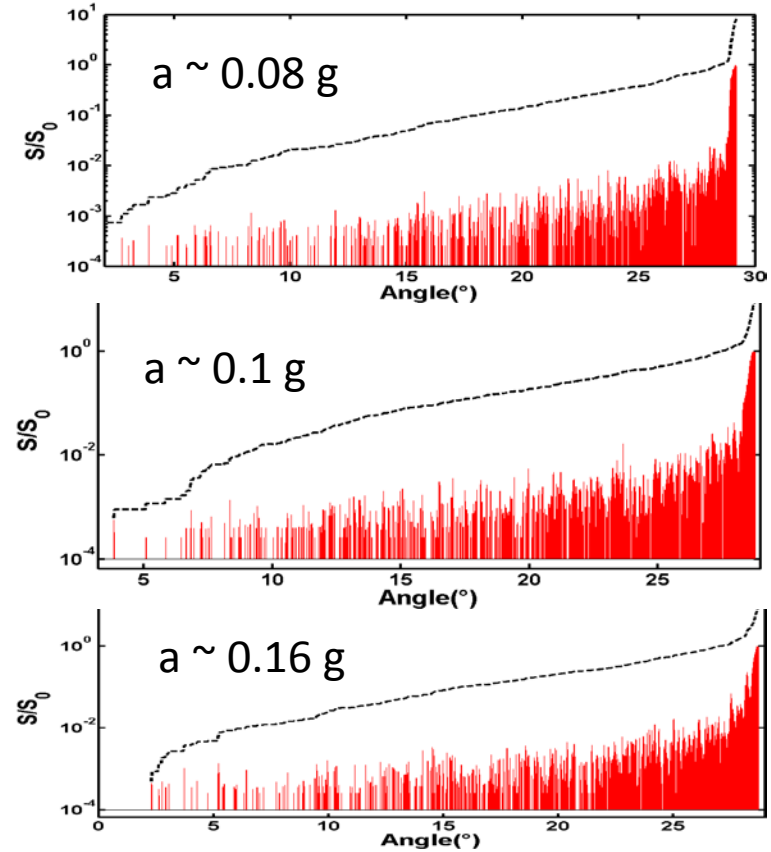
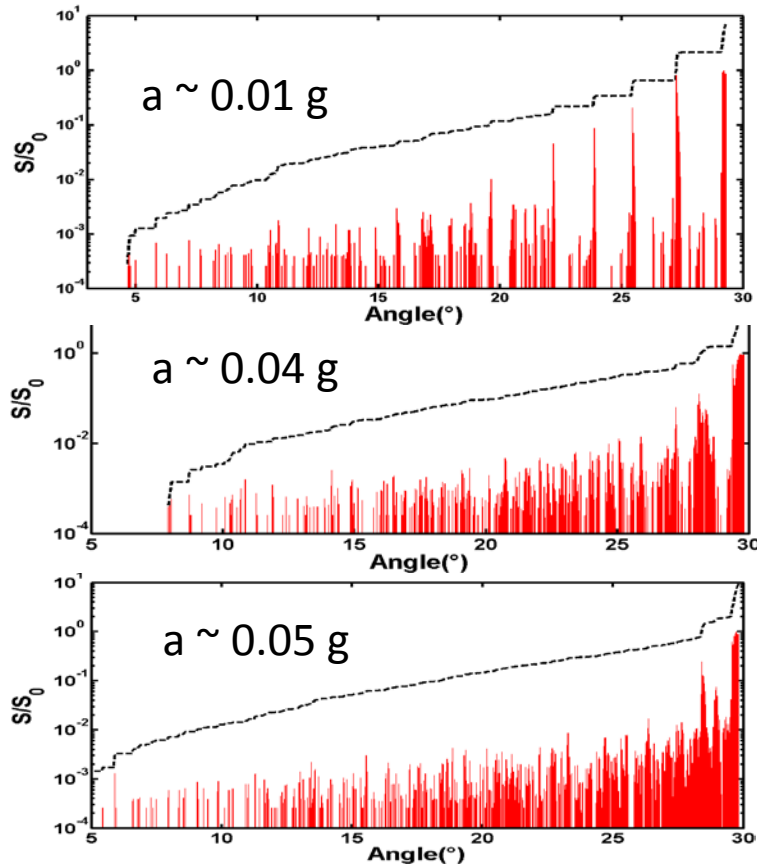


Periodic Pulses
(electrom. exc.)

Accelerometer
measurements

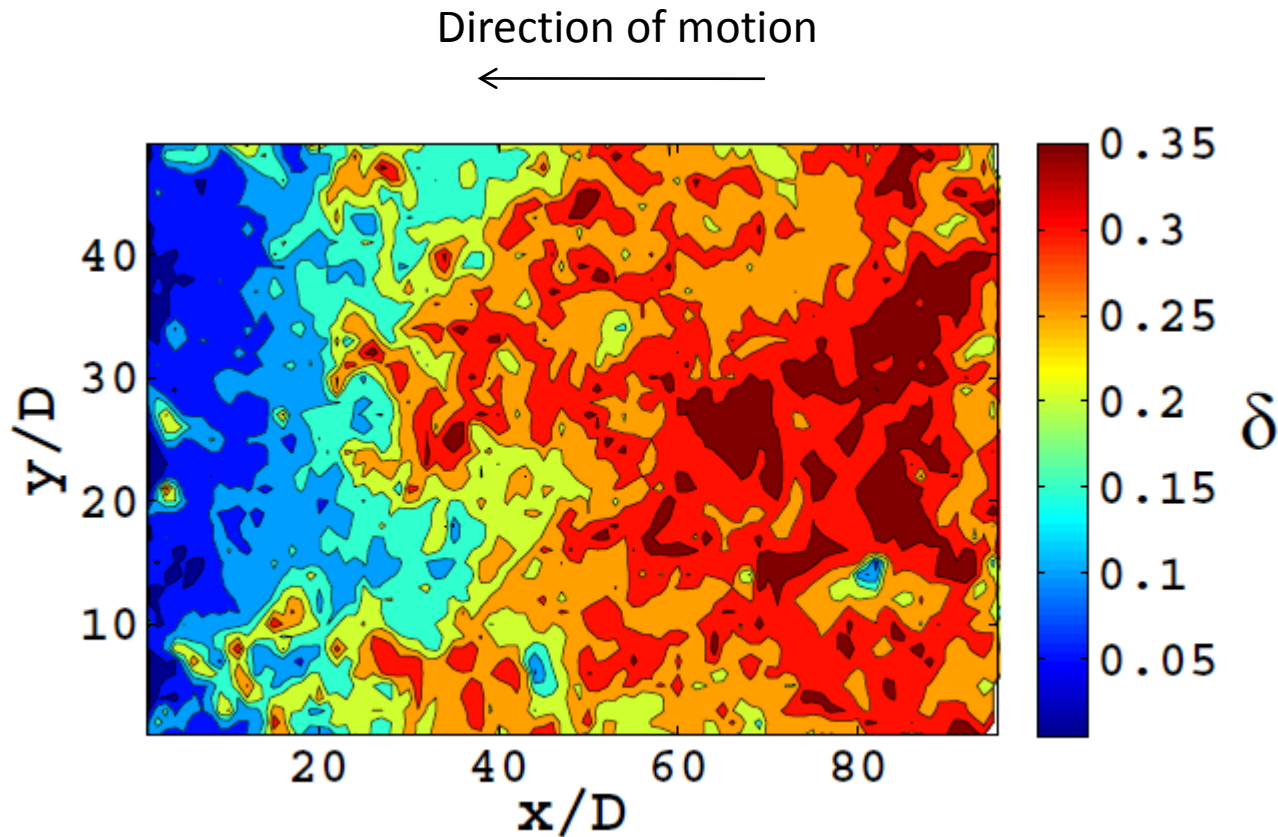


Influence of noise



Precursors are importantly sensitive to mechanical perturbation. Small rearrangement dynamics is very robust.

Displacements during successive precursors

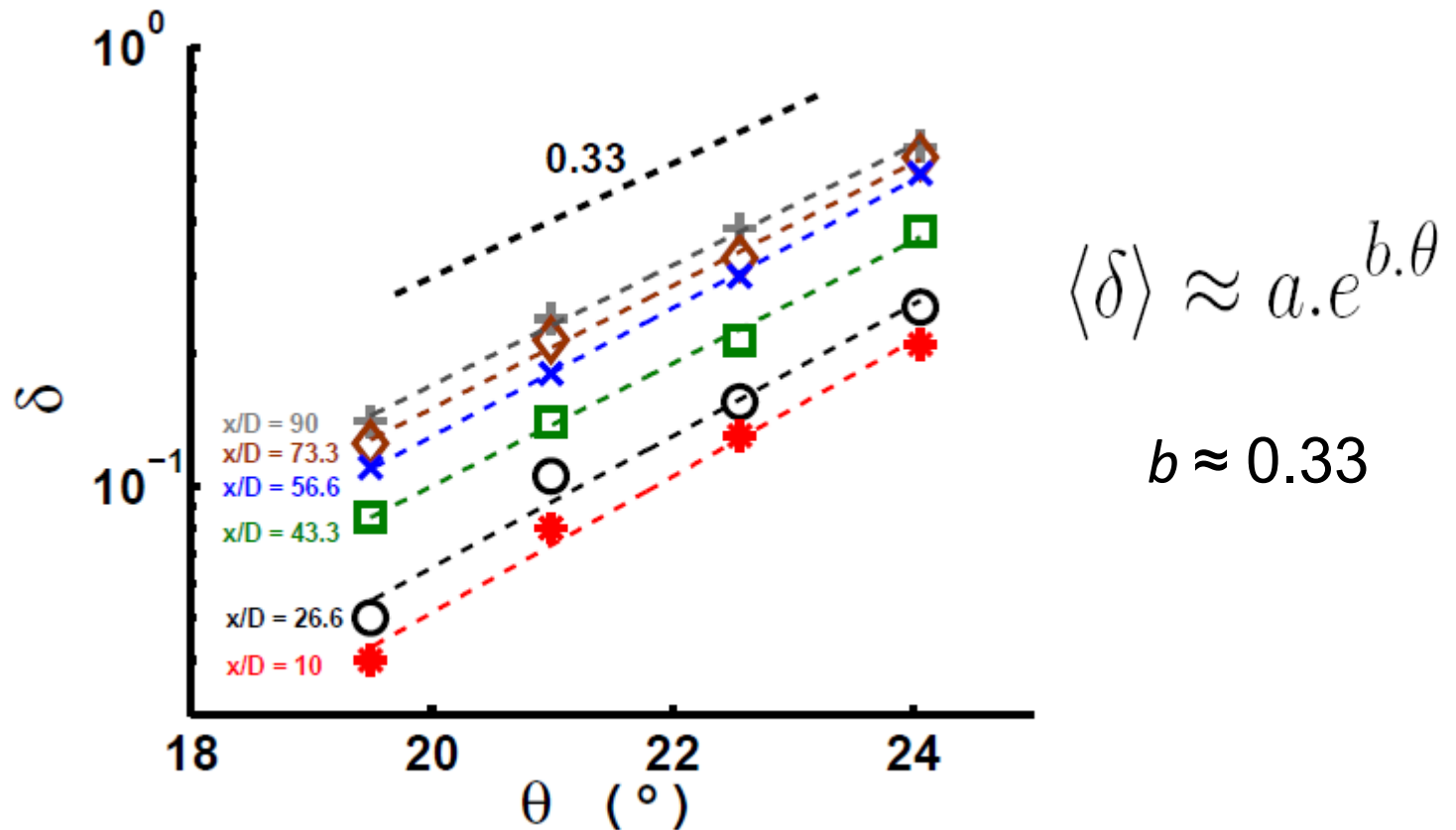


Precursors correspond to successive global mobilizations of grains slipping at the surface of the packing.

Non stationary stick-slip behavior.

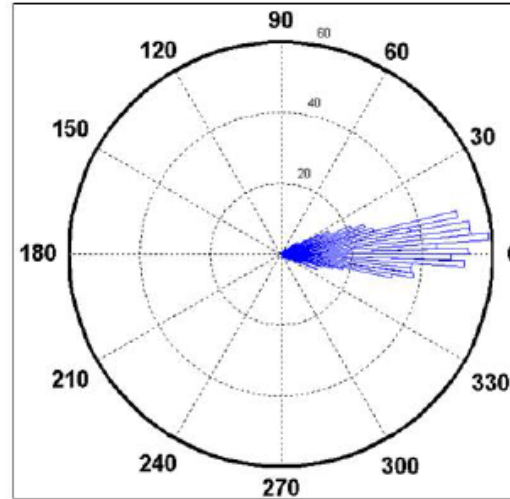
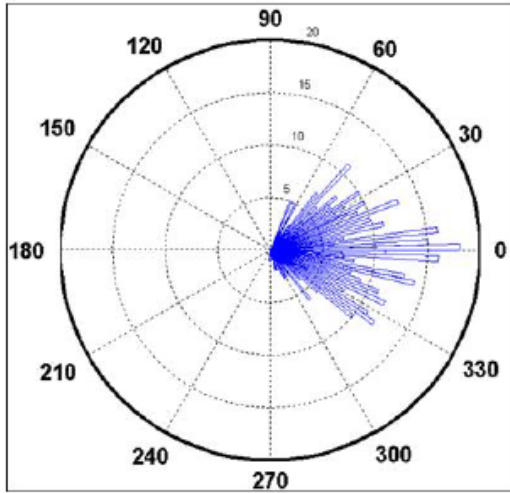
→ Strongly influenced by confinement and boundary cond.

Displacement during 4 consecutive precursors



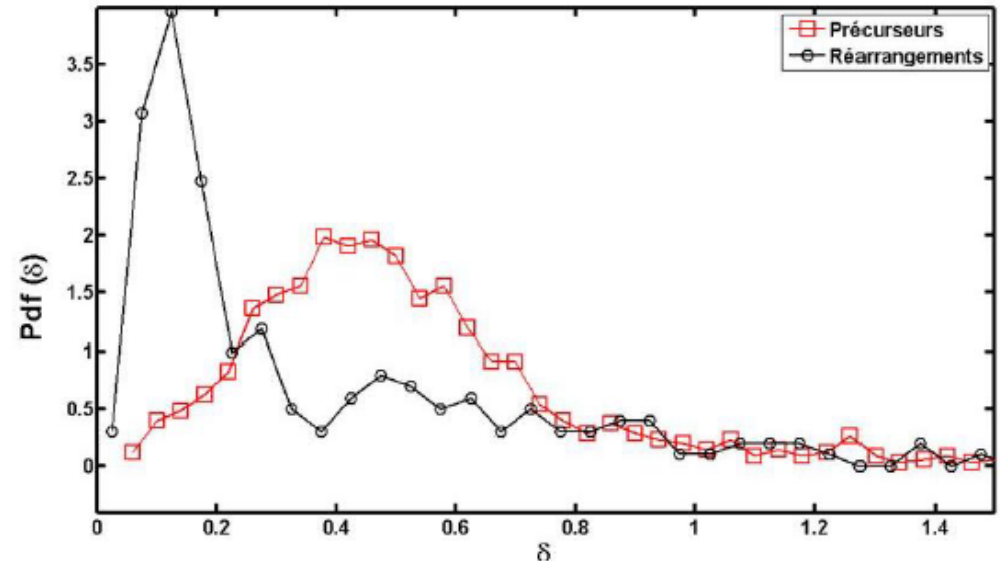
Displacements of grains during precursors increase exponentially during inclination

Displacement of grains

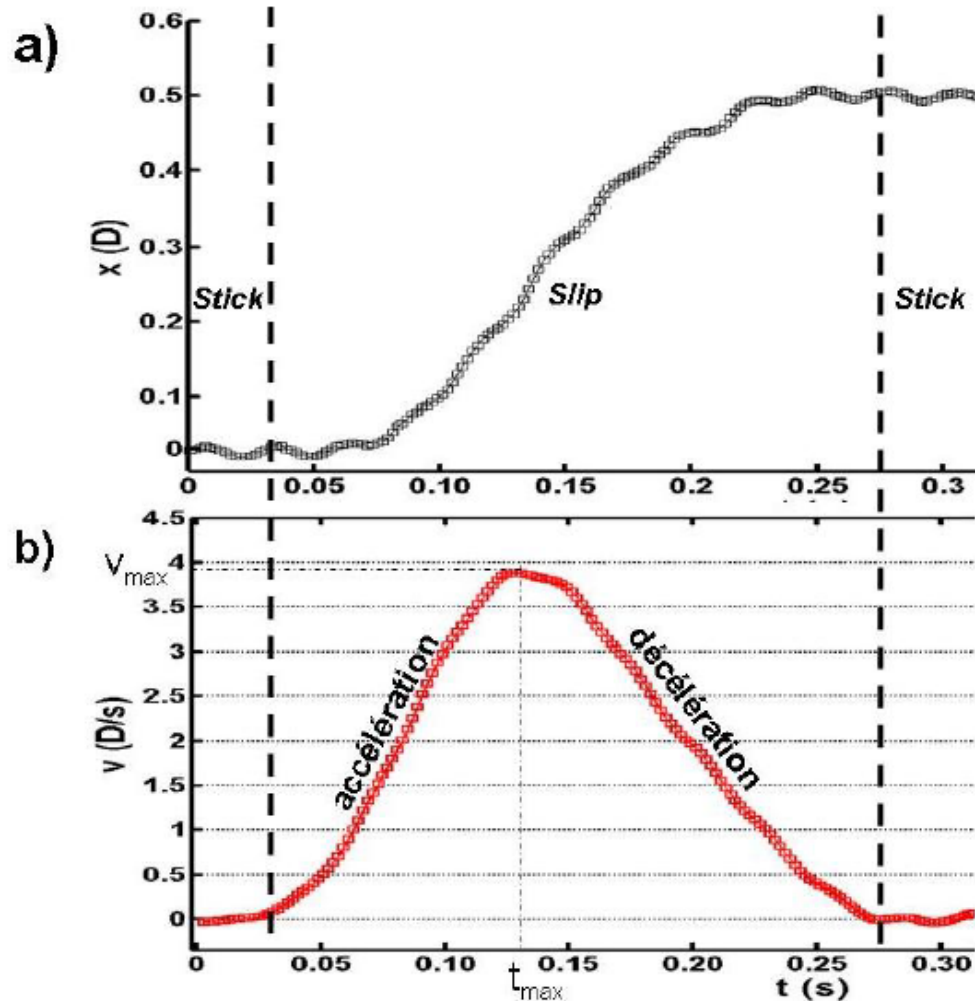


Comparison of the angular distributions of grain displacement vectors during small rearrangements and precursors

- Distribution of the amplitude of grain displacements during rearrangements and precursors. δ is expressed in D units.



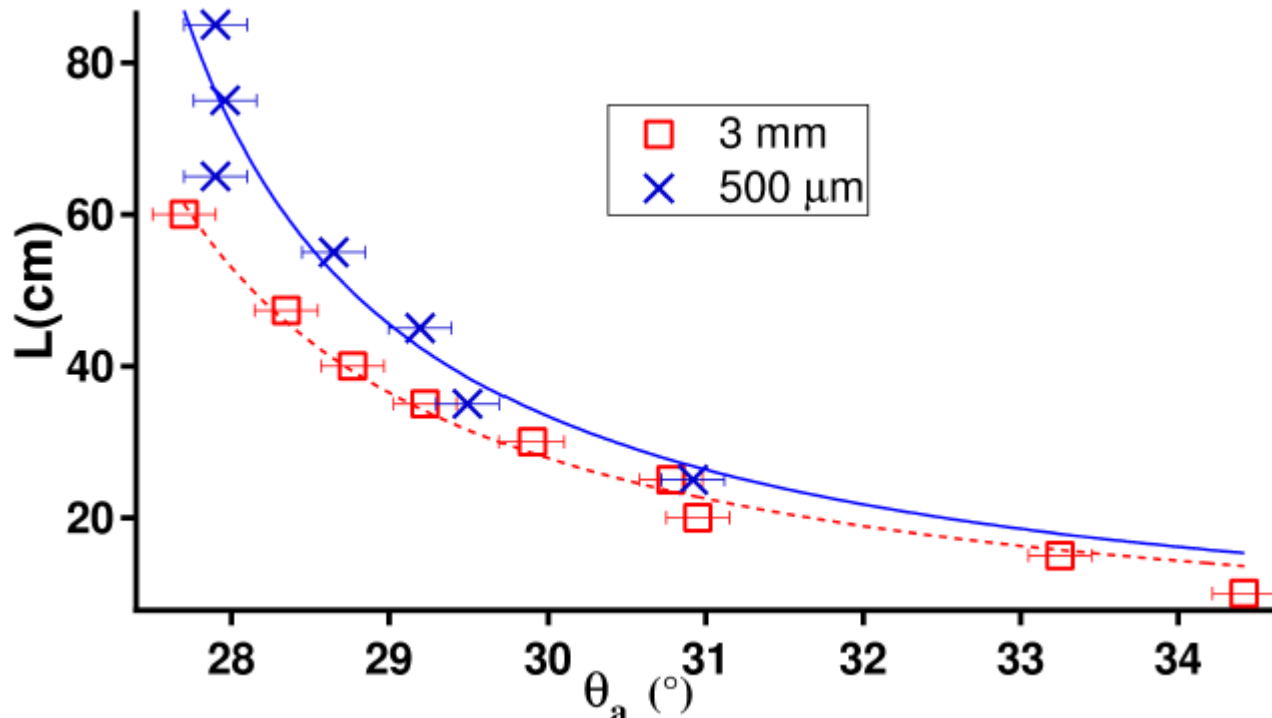
Stick-slip behavior during precursors



- Evolution of the position of a grain during a precursor in function of time.

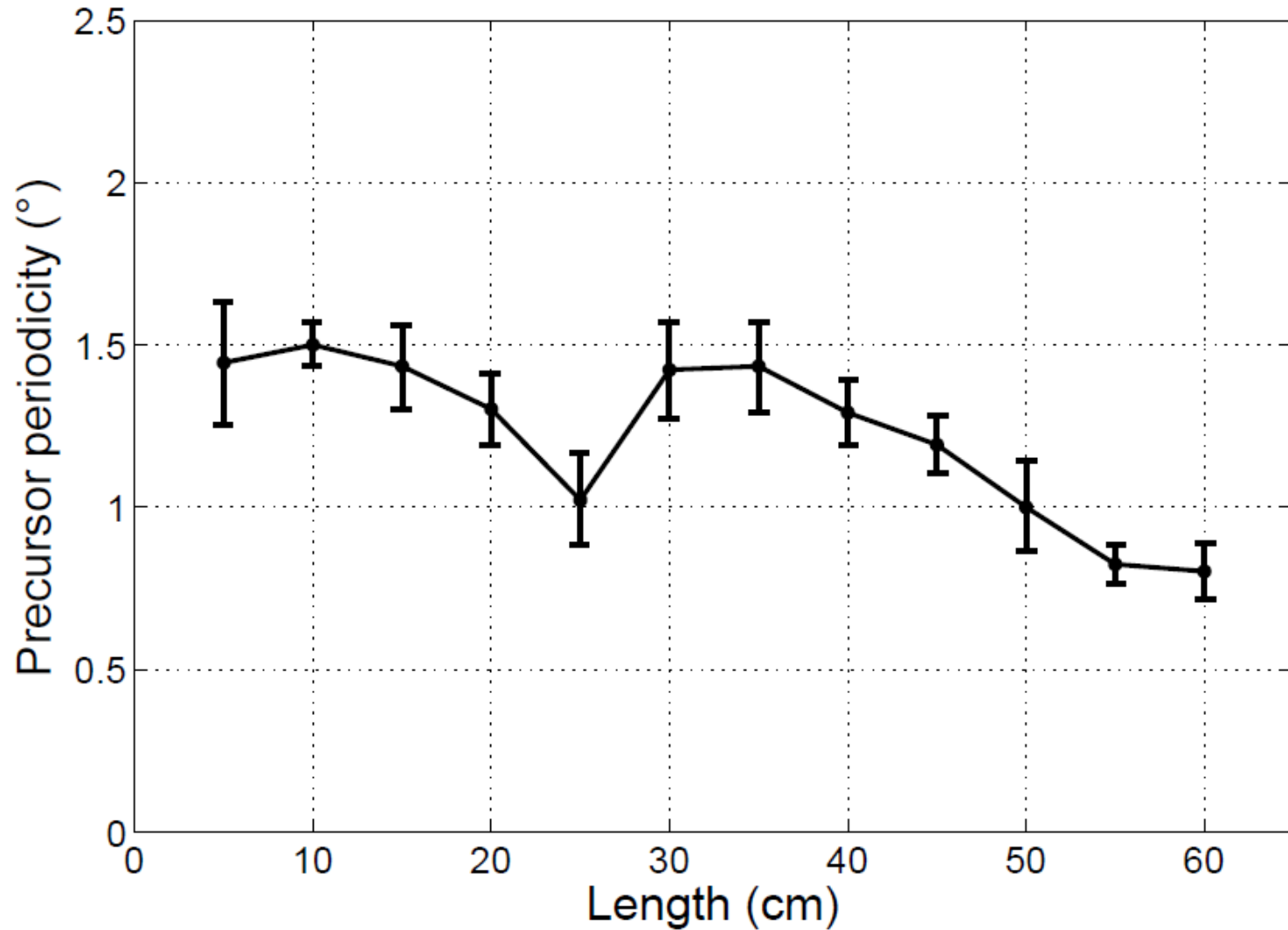
- Evolution of the velocity

Avalanche angle as a function of the box length



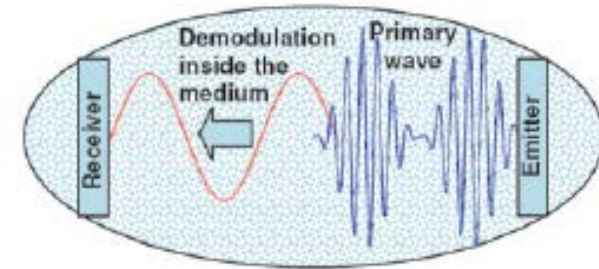
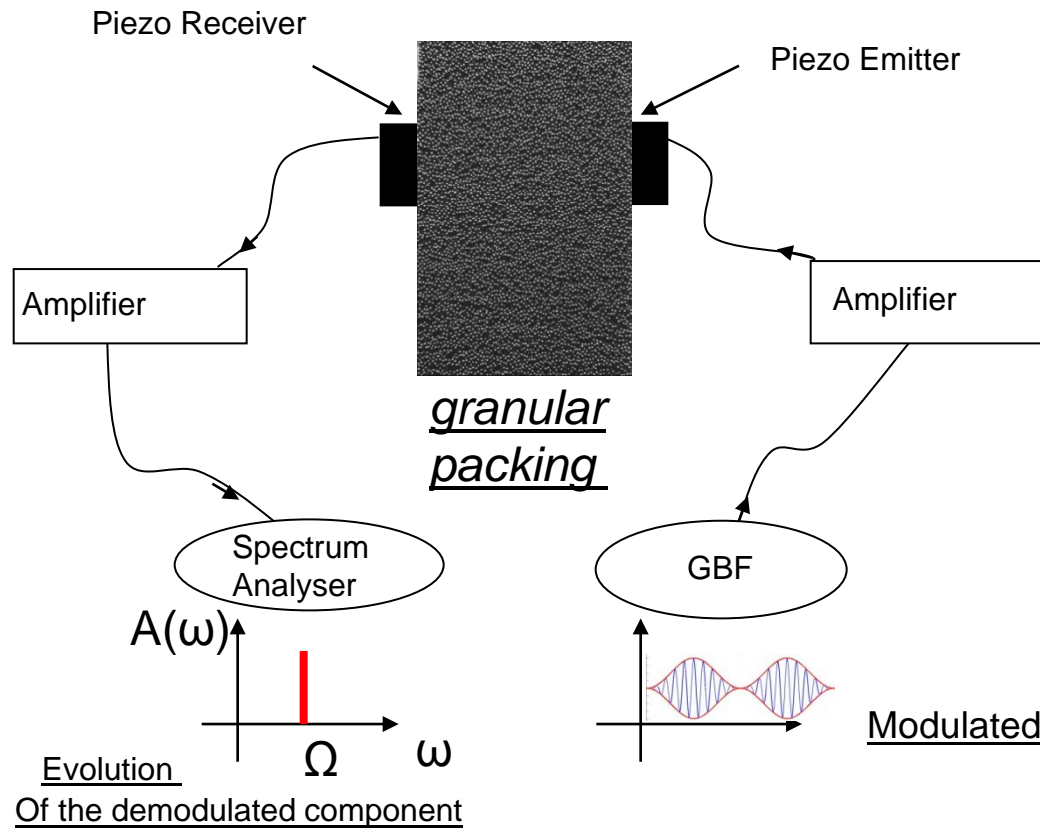
Fit :
$$L = \frac{\frac{\sigma_s}{\rho \cdot g}}{\sin(\theta_a) - \mu_s \cdot \cos(\theta_a)}$$
 (obtained from a simple coulomb criterium : σ_s critical stress, μ_s friction coef.)

Angular interval between successive Precursors as a function of the box length

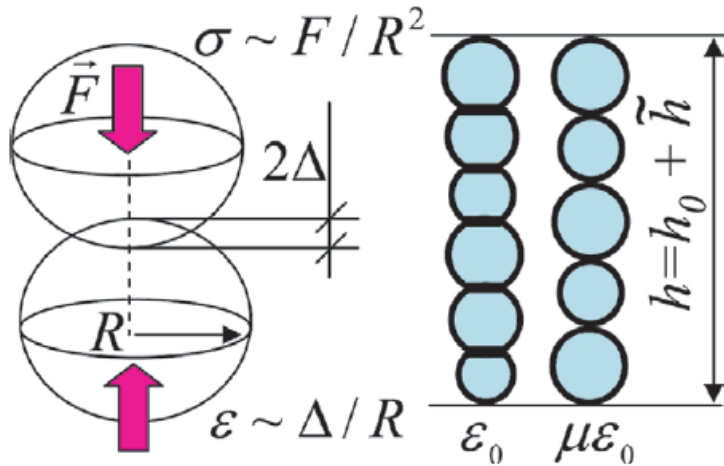


3D experiments : non linear acoustics

V. Zaitsev et al. Europhys. Lett. 83, 64003 (2008)



Non linear acoustics method



Hertzian contact is nonlinear:

$$F = C\Delta^{3/2}H(\Delta)$$

H : Heaviside function

C depends on grain radius R and elastic modulus

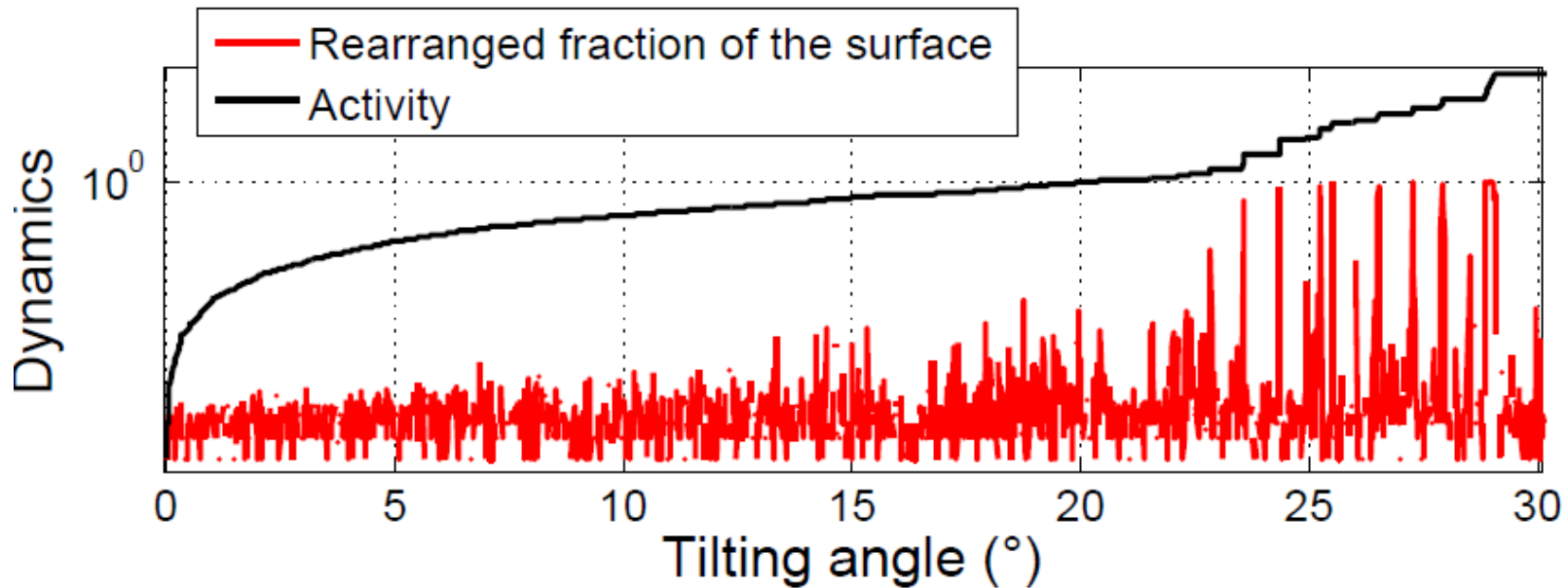
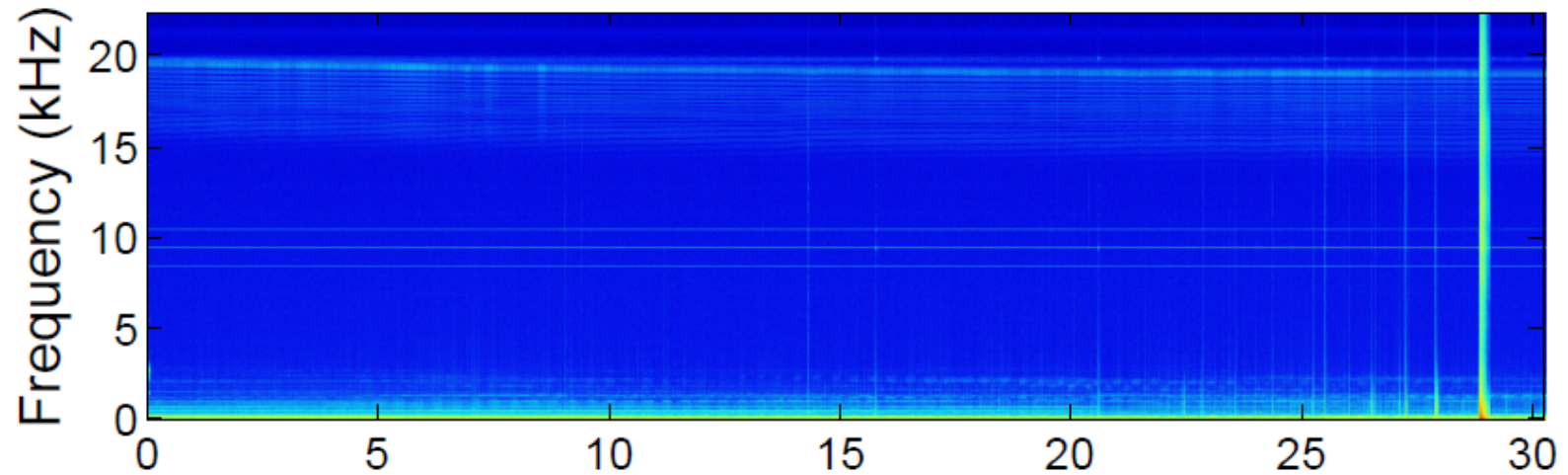
- For a static stress σ_0 , contact chains have different static prestrains ($\varepsilon_0, \mu\varepsilon_0, \mu \ll 1$). The acoustic strain $\tilde{\varepsilon} = \tilde{h}/h_0$ generated by acoustic stress is the same.

- The signal components arising from nonlinearities are dominated by the weakest contact contribution.

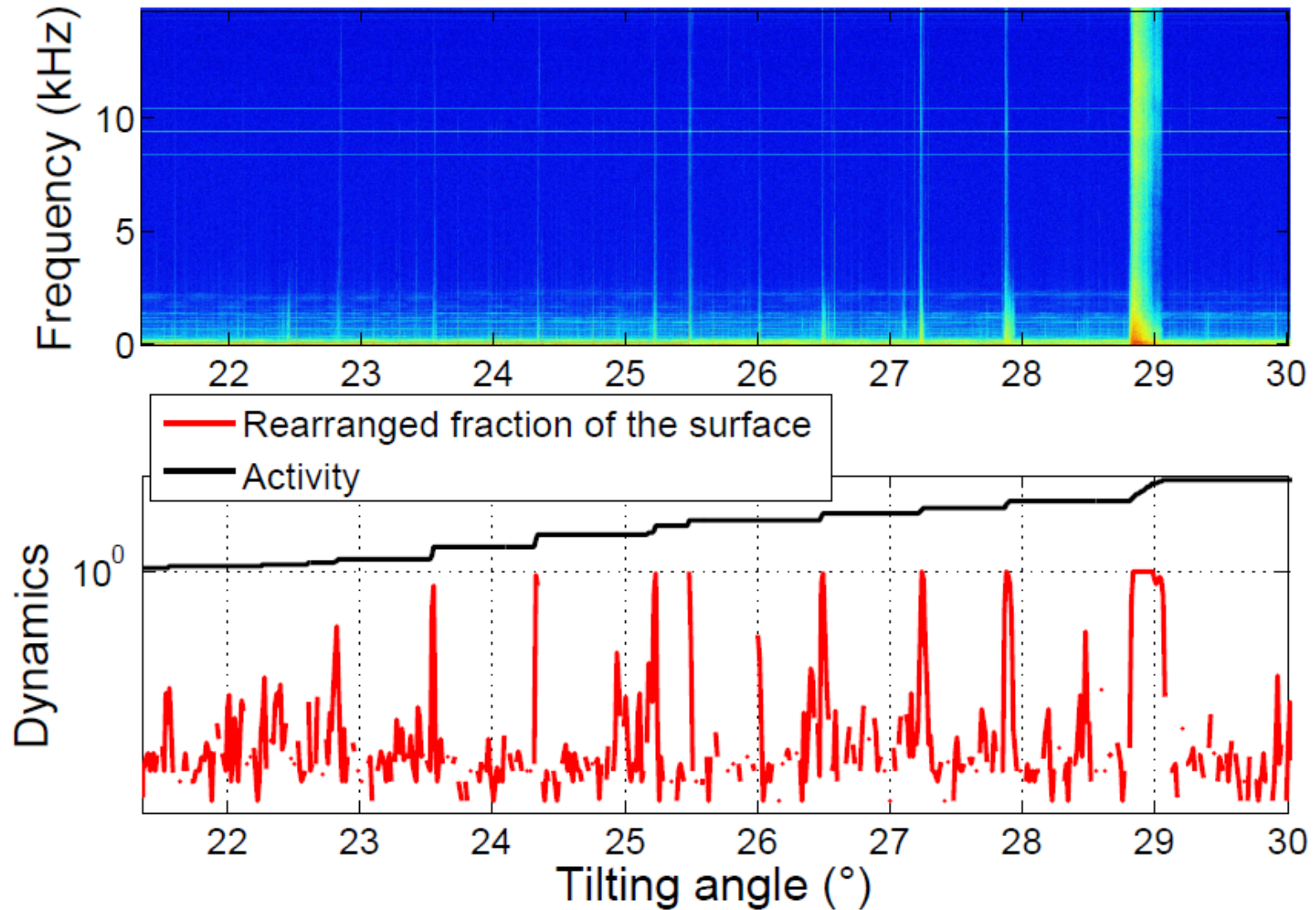
$$\tilde{\sigma}_\omega \propto A\sqrt{\varepsilon_0} \left[1 + \frac{B\sqrt{\mu}}{A} \right] \tilde{\varepsilon}, \quad \tilde{\sigma}_{2\omega, \Omega} \propto \frac{A}{\sqrt{\varepsilon_0}} \left[1 + \frac{B}{A\sqrt{\mu}} \right] \tilde{\varepsilon}^2$$

(A and B : fraction of strong and weak contacts)

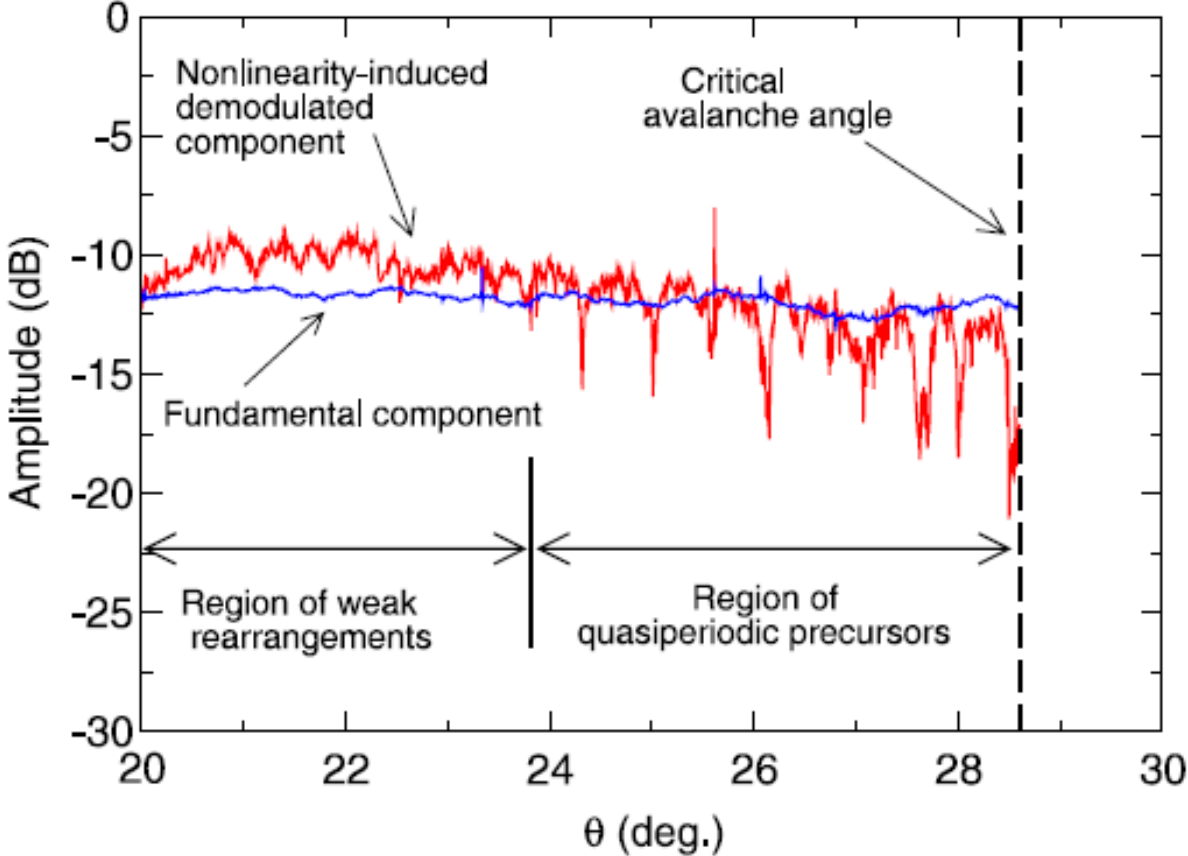
Spectrum



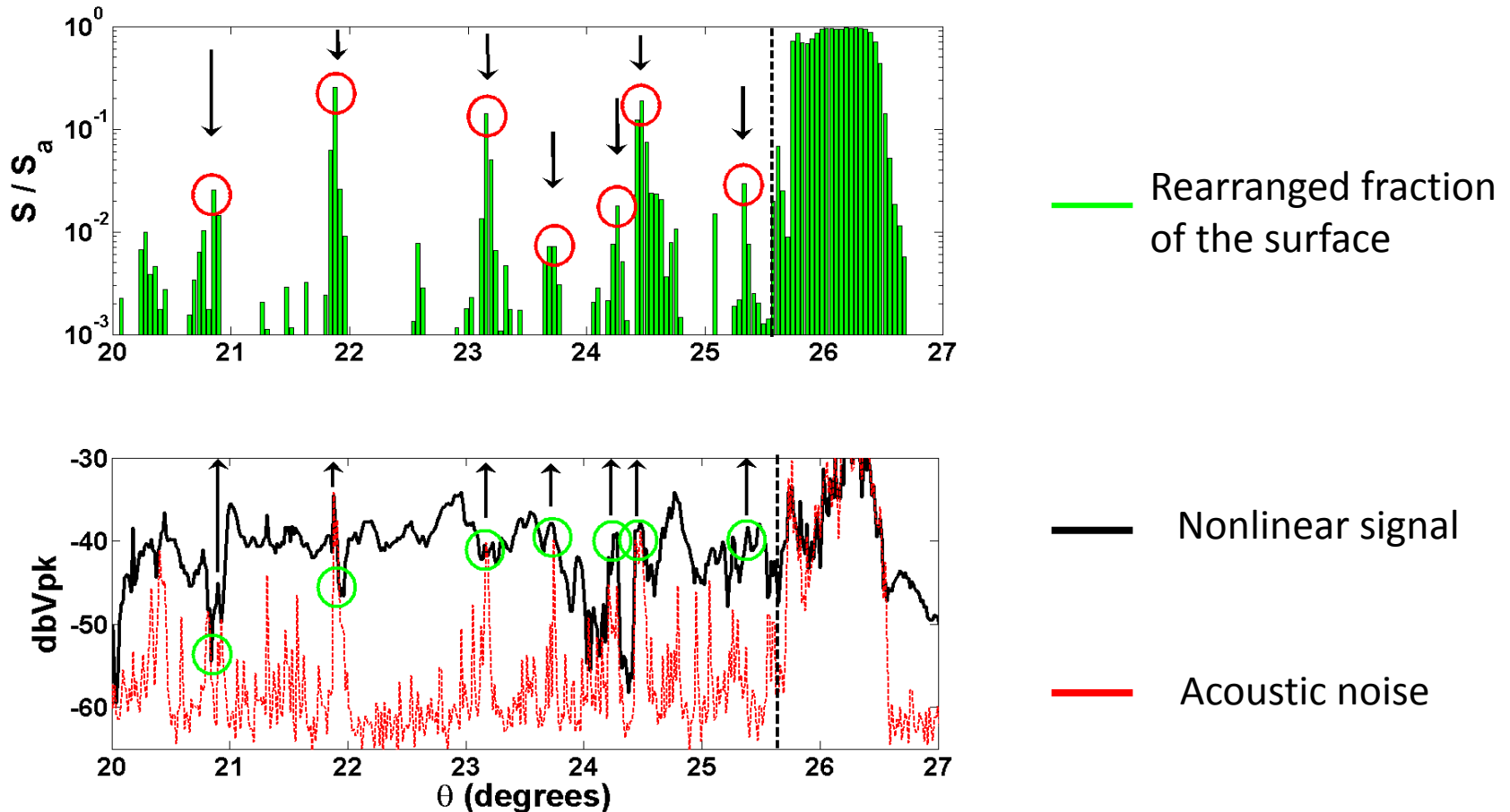
Zoom on the last 10°



Nonlinear signal variability in the precursors regime



Comparative study of the signals

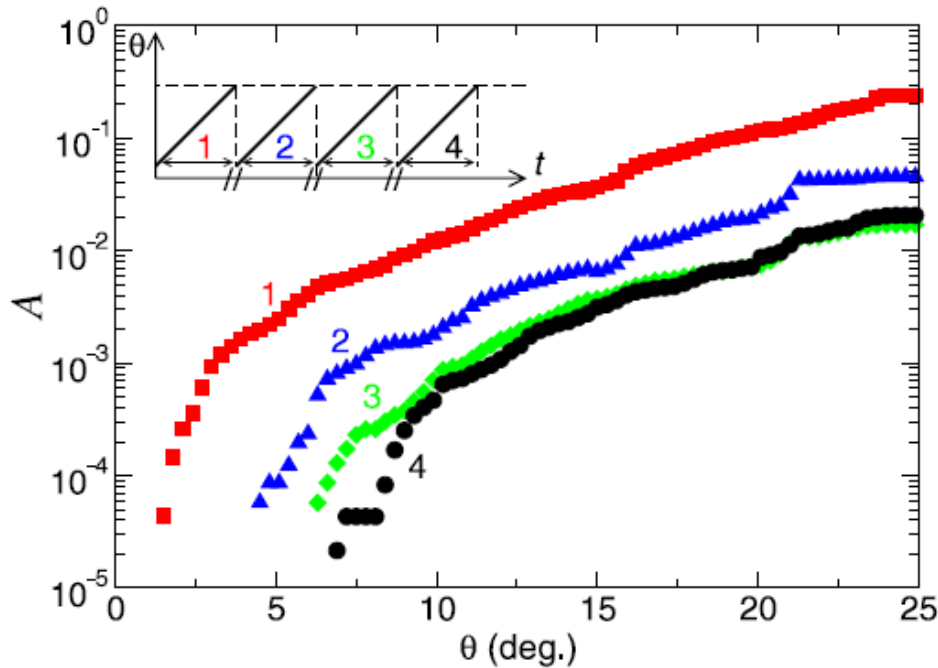


- For some peaks of the surface activity (arrows), rapid variation of non-linear signal
- But : not observed for all the pics and a correspondances are better with noise bursts (used by Gibiat : Journal of acoustical Society of America 2009).

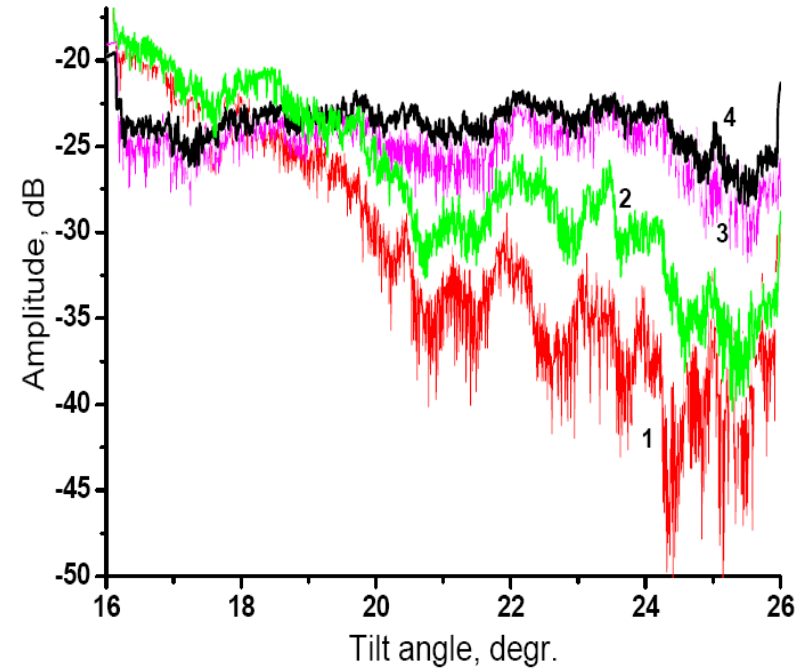
Evidence of ageing during cycles of forth and back tilting.

V. Yu. Zaitsev et al., J. Stat. Mech. P11023 (2010)

Surface activity



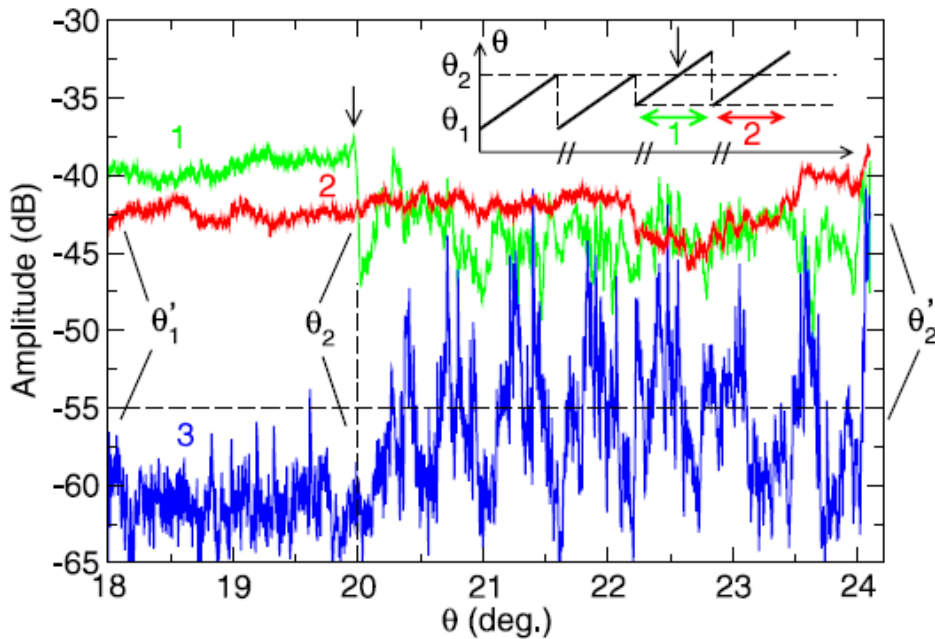
Weak contact network



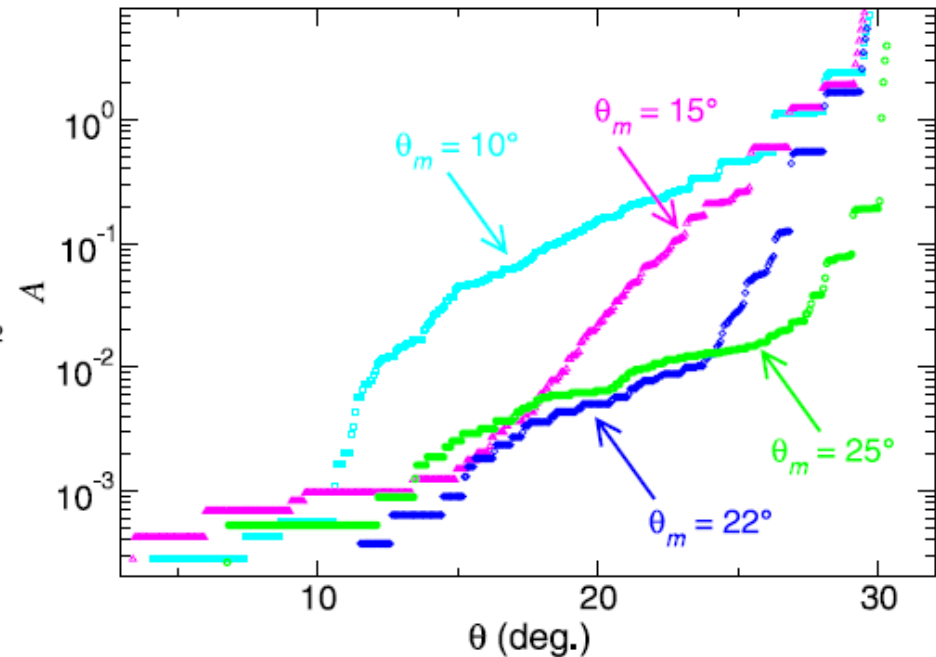
- Surface activity and weak contact modifications decrease to reach a stationary state.
- Strong memory effects
- In good agreement with numerical simulations (S. Deboeuf et al. Phys. Rev. E 2005)

Reactivation upon surpassing the previous upper angle

Weak contact network



Resurgence of surface activity for various ageing angles θ_m



- Aged configurations present reactivation upon surpassing θ_m (weak contact network as well as surface activity)
- Precursors disappear during ageing and reappear with reactivation



End

Les articles de fond ne remontent jamais à la surface.

Boris Vian

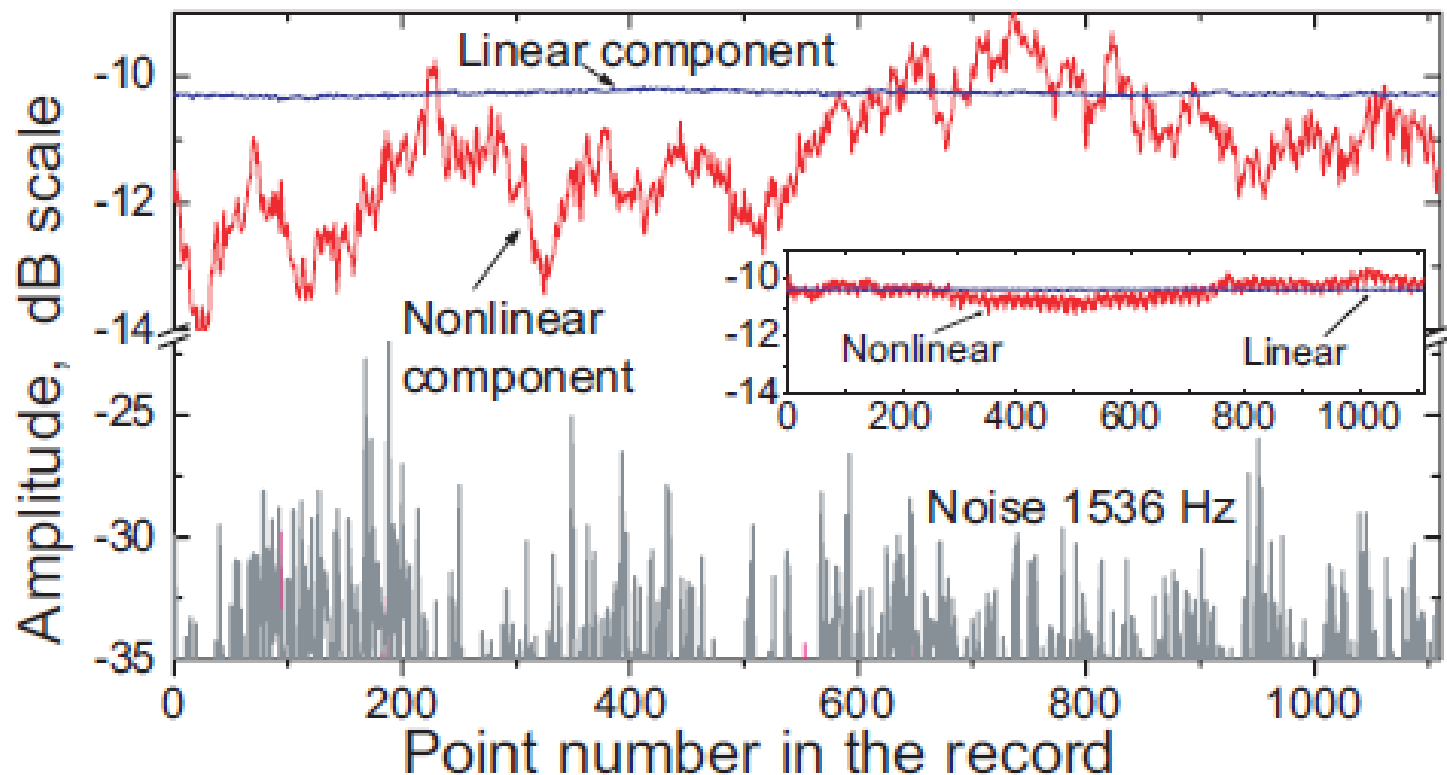


Fig. 7: Pronounced variations in the nonlinear signal recorded 10 min after the avalanche revealing active rearrangements in the apparently motionless packing. The record in the inset (in the same scale) is made 38 min after the avalanche, when the medium has almost reached a new equilibrium (1000 points = 39.05 s).

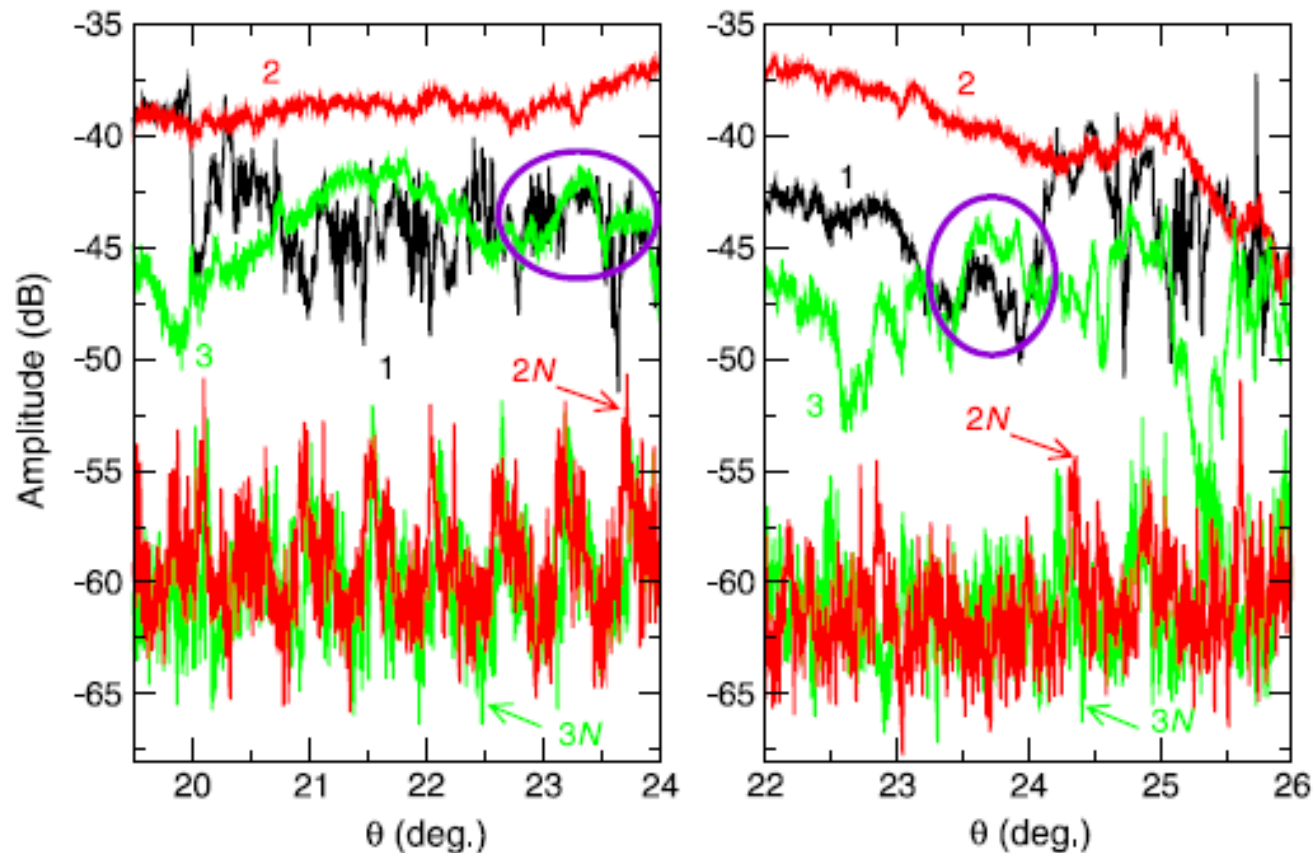


Figure 14. Examples of relaxation of the weak-contact network for two subsequent angular ranges of tilting (bead diameter $d = (2 \pm 0.1)$ mm). Curves 1 are for the first upward tilt in the angular range. Aged curves 2 are recorded after three (left panel) and two (right panel) consecutive up-and-down tilts. Curves 3 are obtained after 20 min (left panel) and 45 min (right panel) of rest at the minimal angle before the next tilt. The noise curves $2N$ and $3N$ correspond to curves 2 and 3, respectively.